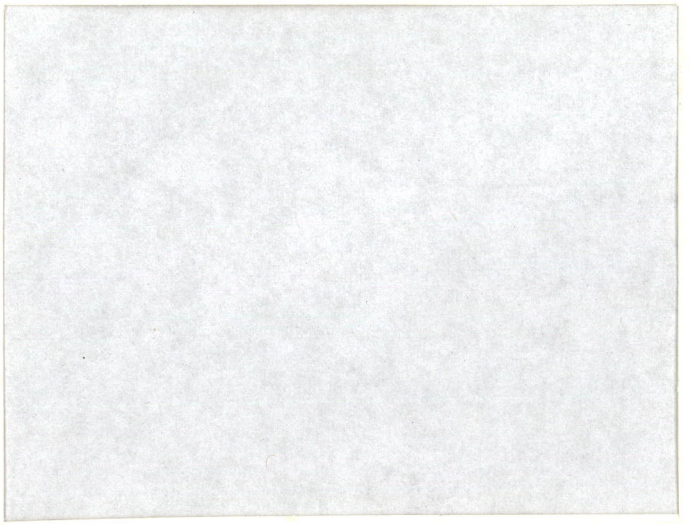

DISCLAIMER

THE EFFECTS OF FINITE SIZE ON THE CRITICAL BEHAVIOR OF FLUID FILMS

by

Benno Abbott Scheibner

A.B., Colgate University, 1970

M.S., University of Colorado, 1975

A thesis submitted to the Faculty of the Graduate School of the University of Colorado in partial fulfillment of the requirements for the degree of Doctor of Philosophy

Department of Physics and Astrophysics

1978

This Thesis for the Doctor of Philosophy Degree by

Benno Abbott Scheibner

has been approved for the

Department of

Physics and Astrophysics

by

_____

Richard C. Mockler

_____

William J. O'Sullivan

Date _____

Scheibner, Benno Abbott (Ph.D., Physics)

The Effects of Finite Size on the Critical Behavior of Fluid Films

Thesis directed by Professors Richard C. Mockler and William J. O'Sullivan

This thesis presents the results of refractive index studies performed on films of a critical mixture of 2,6-lutidine+water near the lower critical point. The films ranged in thickness from 0.46 μm to ~300 μm and were confined between the highly reflecting surfaces of a pair of optical flats in an interferometer. Above the critical temperatures of these films, in the two-phase region, we have measured Δn, the difference between the refractive indexes of the two phases. Since to a close approximation Δn is proportional to the order parameter, measurements of Δn as a function of temperature map out the coexistence curves of the films. For each film of thickness less than 6 μm, we observe a crossover from three dimensional (3d) to two dimensional (2d) scaling behavior. That is, each of these films has a crossover temperature, $T_x(L)$, at which the shape of the coexistence curves change markedly. The data with $T < T_x(L)$ are described by coexistence curves of the form

$$\Delta n = A_2(L)\left(\frac{T - T_{c2}(L)}{T_{c2}(L)}\right)^{\beta_2}$$

with a weighted average value of $\beta_2 = 0.126 \pm 0.005$ in close agreement with the 2d Ising value $\beta_2 = 0.125$. The data with $T > T_x(L)$ are described by coexistence curves of the form

$$\Delta n = A_3 \left(\frac{T - T_{c3}(L)}{T_{c3}(L)} \right)^{\beta_3} \quad ,$$

with a weighted average value of $\beta_3 = 0.332 \pm 0.003$. The dependence of the ratio A_2/A_3 upon film thickness, L, appears to be consistent with the scaling prediction

$$\frac{A_2}{A_3} = E\, L^{(\beta_2 - \beta_3)/\nu_3} \quad ,$$

where ν_3 is the three dimensional correlation length critical exponent.

The following results were extracted from the data for films in the thickness range 0.46 μm < L < 6.0 μm:

$$T_x(L) - T_{c3}(L) = (0.0127 \pm 0.0010) L^{-1/y_3} \quad ,$$

$$T_x(L) - T_{c2}(L) = (0.0264 \pm 0.0016) L^{-1/y_2} \quad ,$$

and

$$T_{c3}(L) - T_{c2}(L) = (0.0129 \pm 0.0012) L^{-1/x} \quad ,$$

where $y_3 = 0.66 \pm 0.06$, $y_2 = 0.61 \pm 0.06$, and $x = 0.64 \pm 0.09$. L is measured in μm, while the temperature units are degrees Kelvin. To within the experimental precision each of the exponents is equal to ν_3. $T_{c2}(L)$ is the 2d critical temperature (where phase separation occurs), while $T_{c3}(L)$ is a 3d critical temperature defined by extension of the 3d coexistence curve into the 2d region. The above results suggest that $(T_x - T_{c3}) = (T_{c3} - T_{c2})$.

Critical temperatures were measured for films ranging in thickness from 0.46 μm to 280 μm. For films confined between silver-coated surfaces we found

$$T_{c3}(L) - T_{c3}(\infty) = +(0.047\pm0.002)L^{-(0.81\pm0.08)} ,$$

while for films confined between SiO_2 overcoated dielectric surfaces we found

$$T_{c3}(L) - T_{c3}(\infty) = -(0.24\pm0.05)L^{-(0.80\pm0.09)} .$$

The exponent describing the shift in critical temperature appears to be the same for both sets of surfaces. However, the magnitudes and signs of the $T_{c3}(L)$ shifts are different for the two surfaces.

This abstract is approved as to form and content. I recommend its publication.

Signed _____

_____

Faculty members in charge of dissertation

ACKNOWLEDGMENTS

I would like to thank my thesis advisors, Dick Mockler and Bill O'Sullivan, for their patience, interest, and concern.

My fellow graduate students have always proven to be good listeners and have provided valuable assistance. In particular, Mike Meadows has participated in many helpful discussions. Mark Handschy made several of the measurements necessary for this work. Don Jacobs' pioneering experiments made this work possible.

It is impossible to thank my parents adequately for thirty years of support and encouragement.

I would like to thank my wife, Barbara, for her patience. She has been forced to postpone many of her own dreams, in order that this work could be completed.

My daughter, Cassandra, has shown considerable interest in my work. This volume is dedicated to her in hope that someday there may be more women physicists.

TABLE OF CONTENTS

CHAPTER		PAGE
I.	INTRODUCTION	1
	1.1 Purpose	1
	1.2 Review of previous theoretical and experimental work	6
II.	EXPERIMENTAL APPARATUS	9
	2.1 Cell design and use	9
	2.2 Temperature control	11
	2.3 Fluids	13
III.	EXPERIMENTAL PROCEDURE	16
	3.1 Film preparation	16
	3.2 Finding T_c	18
	3.3 Measurement of Δn	21
IV.	COEXISTENCE CURVE ANALYSIS	27
	4.1 Lorentz-Lorenz relation	27
	4.2 Qualitative discussion of the data	28
	4.3 Details of fitting procedure	30
V.	RESULTS	35
	5.1 Coexistence curves	35
	5.2 $[T_{c3}(L)-T_{c2}(L)]$ results	43
	5.3 Crossover points	47
	5.4 Critical temperature shifts	54
	5.5 Results with dielectric coatings	58

CHAPTER PAGE

VI. SUMMARY AND OUTLOOK 63

6.1 A summary of our results 63

6.2 Outlook for future work 67

BIBLIOGRAPHY 69

APPENDIX 71

LIST OF TABLES

TABLE		PAGE
I.	Values for β_3 and A_3 found with silver surfaces	39
II.	Values for β_2 and A_2 found with silver surfaces	41
III.	Values for T_{c3} and T_{c2} found by fitting silver data	46
IV.	Values for T_x found with silver surfaces	48
V.	Values for T_{c3} found with silver surfaces	56
VI.	Values for T_{c3} found with dielectric coated surfaces	60

LIST OF FIGURES

FIGURE		PAGE
1.	Apparatus (a) and view through telescope (b)	5
2.	Experimental cell	10
3.	A wedge of fluid trapped between the optically flat surfaces	23
4.	Typical Δn versus temperature measurements	29
5.	Critical exponent β_3 versus film thickness	36
6.	Coexistence curve coefficient A_3 versus film thickness	37
7.	Critical exponent β_2 versus film thickness	40
8.	Coexistence curve coefficient A_2 versus film thickness	42
9.	Reduced coexistence curve coefficient A_2' versus film thickness	44
10.	$[T_{c3}(L)-T_{c2}(L)]$ versus film thickness	45
11.	$[T_x(L)-T_{c3}(L)]$ versus film thickness	50
12.	$[T_x(L)-T_{c2}(L)]$ versus film thickness	51
13.	A_2/A_3 versus film thickness	53
14.	$[T_{c3}(L)-T_{c3}(\infty)]$ versus film thickness for silver surfaces	55
15.	$[T_{c3}(\infty)-T_{c3}(L)]$ versus film thickness for dielectric coated surfaces	61

CHAPTER I

INTRODUCTION

1.1 Purpose

Critical phenomena are observed in binary liquid mixtures, ferromagnets, liquid-gas systems, liquid helium, and superconductors. It is surprising that such diverse systems all display behavior that can be described in the same terms. Each of these systems has a critical temperature, T_c, at which a transition occurs. Near these critical points certain thermodynamic properties of the systems appear to diverge. These divergences can be characterized by critical exponents. Experimentally it has been found that for many different systems the critical exponents have values that are apparently equal. The concept that broad classes of systems have identical critical exponents is called universality. In this thesis we report the results of measurements made on a binary liquid mixture, 2,6-lutidine+water, near its lower critical point. Consequently, we shall discuss the critical behavior of that particular system in some detail. It should be kept in mind, however, that universality predicts similar behavior in other related critical systems.

At room temperature lutidine and water are completely miscille. A mixture of the two fluids with a concentration of 28.7% by weight lutidine is a critical mixture. As the temperature of a bulk

sample of the critical mixture is raised from room temperature the fluids remain mixed, in one phase, until the critical temperature, 34 C, is reached. At that temperature a meniscus appears, separating two fluid phases. The upper phase has a higher concentration of lutidine than the lower phase. If the temperature is raised further the relative lutidine concentrations in the two phases changes. The difference in lutidine concentration is a function of $T-T_c$ and is given by the coexistence curve, which is characterized by the critical exponent β. Binary fluid mixtures are Ising type systems (Greer, 1976) and so $\beta \approx 1/3$. We have described the transition at the lower critical point of lutidine+water. If we continue to raise the temperature of the mixture we eventually reach an upper critical point temperature where the meniscus disappears and the fluids mix again into a single fluid phase.

Near the critical temperatures of binary liquid mixtures critical opalescence is observed. That is, the fluids display a milky iridescence when illuminated. This opalescence is due to fluctuations in the fluids which scatter visible light strongly. Fluctuations occur in all critical systems and play a central role in the anomalous behavior near critical points. The size of a typical fluctuation is given by the correlation length, $\xi = \xi_o \varepsilon^{-\nu}$, with $\varepsilon = (T-T_c)/T_c$. For Ising systems ν is approximately 2/3.

In the past decade remarkable progress has been made experimentally and theoretically in understanding the properties of bulk critical systems, such as that described above. Most

critical phenomena experiments are performed using samples of macroscopic size. The physical dimensions of the sample are much larger than the correlation length at all accessible temperatures. In addition, in most experiments an insignificant fraction of the molecules is in contact with the walls of the sample container. Thus, most investigations of critical behavior can ignore finite size and bounding surface effects. The experiment which forms the basis of this thesis has been designed specifically to investigate these effects.

In this thesis we present the results of refractive index measurements made on films of a critical mixture of lutidine and water. The films ranged in thickness from 0.46 μm to 300 μm, and were confined between the coated surfaces of a pair of optical flats. For these films the correlation length can become comparable to the film thickness at temperatures close to the critical temperature. The bounding surfaces limit the growth of fluctuations in one dimension and as the temperature of a film is brought very close to the critical temperature the correlation length can only increase in two dimensions. Since the fluctuations play a decisive role in the critical behavior it is conceivable that under the above conditions crossovers from three dimensional to two dimensional critical behavior may occur.

The critical behavior of films may differ from the behavior of bulk samples in a second way. In a bulk sample the surface contributions to the free energy of the system can be ignored. In a film the enhanced surface-to-volume ratio makes these surface

terms much more important. Thus the free energy per molecule for a film may be significantly different than for a bulk sample. Since the critical temperature of a system is directly related to the average free energy per molecule, the critical temperature of a film may be shifted relative to that of a bulk sample.

Both of the finite size effects described above have been observed in our experiment. Furthermore, we have been able to study the dependence of the crossover behavior and the critical temperature shifts upon film thickness.

A schematic diagram of the apparatus used in our experiment is shown in Fig. 1a. The fluid films lie between the coated surfaces of the optical flats in a temperature controlled cell. The spacing between the flats can be adjusted allowing us to study films ranging in thickness from 0.4 μm to 300 μm. When expanded and collimated light from a He-Ne laser illuminates the flats at normal incidence, equal thickness fringes are formed. The positions of these fringes were measured with a telescope mounted on a traveling micrometer stage. At small spacings, in the two-phase region, drops consisting of the separated phases form between the flats and are immobile. (These drops are easily seen when viewed in white light.) Since the two phases have slightly different refractive indexes they cause fringes to appear at different points, and the fringes appear to split as shown in Fig. 1b. Measurement of this splitting allows us to calculate Δn, the difference in index of refraction between the two phases. From the Lorentz-Lorenz relation it can be shown that measurements of Δn as a function of

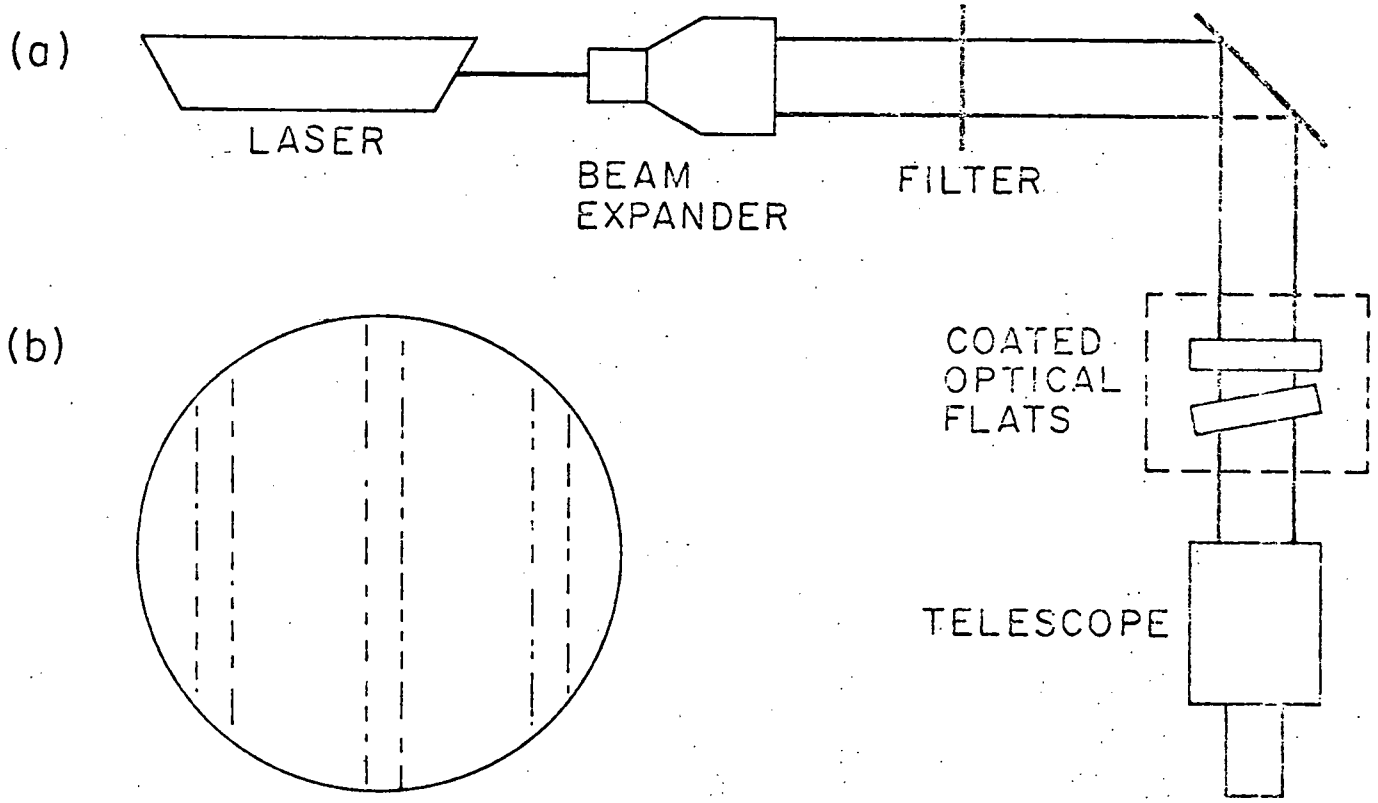

Fig. 1. Apparatus (a) and view through telescope (b).

temperature map out the coexistence curve (Jacobs et al., 1977). Thus we were able to measure the coexistence curve at a variety of film thicknesses.

1.2 Review of previous theoretical and experimental work

Fisher (1971 and 1973) has discussed the expected behavior of critical films in some detail. Although his arguments have been made for crossovers in the one-phase region they can easily be applied to crossovers in the two-phase region. It is presumed that each film of thickness L will have a crossover at a temperature $T_x(L)$. $T_x(L)$ separates two dimensional (2d) and three dimensional (3d) temperature regimes. In the 3d regime the properties of a film should be indistinguishable from those of a bulk sample. In the 2d regime however, the critical properties of a film should be characterized by the appropriate 2d critical exponents, with amplitudes that depend upon L.

Crossovers should occur when the correlation length is comparable to the film thickness, or when $L = m\xi$, where m is on the order of unity. Inserting the explicit form for the correlation length in this relation we find that $T_x(L)$ should depend upon L in the following way, $[T_x(L)-T_c(L)] = DL^{-1/\nu_3}$, where $D = T_c(L)[m\xi_o]^{1/\nu_3}$. For crossovers in the two-phase region ν should be replaced by ν'. Throughout this thesis we assume that $\nu = \nu'$ and use the two interchangeably. Our results support this contention.

Fisher (1971 and 1973) has suggested that the shift in critical temperatures for films should have the form

$[T_c(L)-T_c(\infty)] = FL^{-\lambda}$. Scaling theory suggests that $\lambda = 1/\nu$, however Ising lattice calculations indicate that λ is approximately unity for free or hard wall boundary conditions (Binder, 1972 and Domb, 1973).

To put our work in perspective some other experimental work should be mentioned. Two dimensional scaling behavior has been observed in bulk sample antiferromagnets characterized by highly disparate inter- and intra-plane exchange interactions (Shirane and Birgeneau, 1977). In particular, the crystal K_2CoF_4 has proven to behave as a 2d Ising ferromagnet and neutron scattering experiments give 2d critical exponents agreeing closely with those obtained from the Onsager 2d Ising model (Ikeda and Hirakawa, 1974). Although these systems are very different than our films, these results indicate that 2d and in particular 2d Ising behavior can occur in nature. An indication of a possible crossover has been observed in Rb_2FeF_4 (Birgeneau, Guggenheim, and Shirane, 1970). This system belongs to a different universality class than our fluid films, and the mechanism underlying the crossovers is quite different than in our films, however these results show that crossovers in dimensionality are possible.

Resistivity measurements of Ni films ranging in thickness from 200 Å to 13,000 Å show a shift in critical temperature and yield the value $\lambda = 1.33$ (and if $\lambda = 1/\nu_3$, $\nu_3 = 0.75$) (Lutz et al., 1974). Specific heat measurements on liquid helium films show a shift in the superfluid λ-transition temperature with thickness. By such measurements Chen and Gasparini (1978) have found $\lambda = 1.7$ with a

corresponding $\nu_3 = 0.54$. Again these systems belong to different universality classes than our binary liquid films. These experiments do indicate though that critical temperatures can depend upon film thicknesses.

A previous study of finite size effects on fluid film critical behavior was carried out by Jacobs et al. (1976). They observed a dependence upon film thickness of the critical temperature of trapped films of a methanol+cyclohexane critical mixture. In addition, they developed the refractive index technique for mapping out the coexistence curves of critical fluid films. However, only a limited amount of data was taken and no firm conclusions could be drawn. In our experiment we have used the apparatus of Jacobs et al. with only a few modifications. Major improvements in procedure and method of analysis have been made however.

CHAPTER II

EXPERIMENTAL APPARATUS

2.1 Cell Design and Use

Figure 2 is a diagram of the cylindrical sample cell. An optical flat is mounted on axis in each half of the stainless steel cell. The critical fluid mixture is contained between the coated surfaces of the flats and partially fills an adjacent reservoir. The two halves of the cell are connected by a stainless steel bellows and three sets of differential screws. This permits adjustment of the spacing and wedge angle between the flats. The thickness of the fluid film between the flats can thus be adjusted from less than a micron to approximately 300 microns. Caps containing heaters are attached to the two ends of the cell and heavy wire mesh (not shown in Fig. 2) is wound around the outside of the cell to give better thermal contact between the two halves.

The cell is mounted with the optical axis horizontal inside an aluminum heat shield which in turn is mounted inside a vacuum can. Windows (not shown in Fig. 2) in the cell end caps, heat shield and vacuum can permit observation of the flats and fluid while reducing heat losses from the cell. Retractable rods permit adjustment of the differential screws after assembly.

The optical flats used are 1.59 cm in diameter and were flat to $\lambda/100$ before being sealed in the cell. After mounting, the

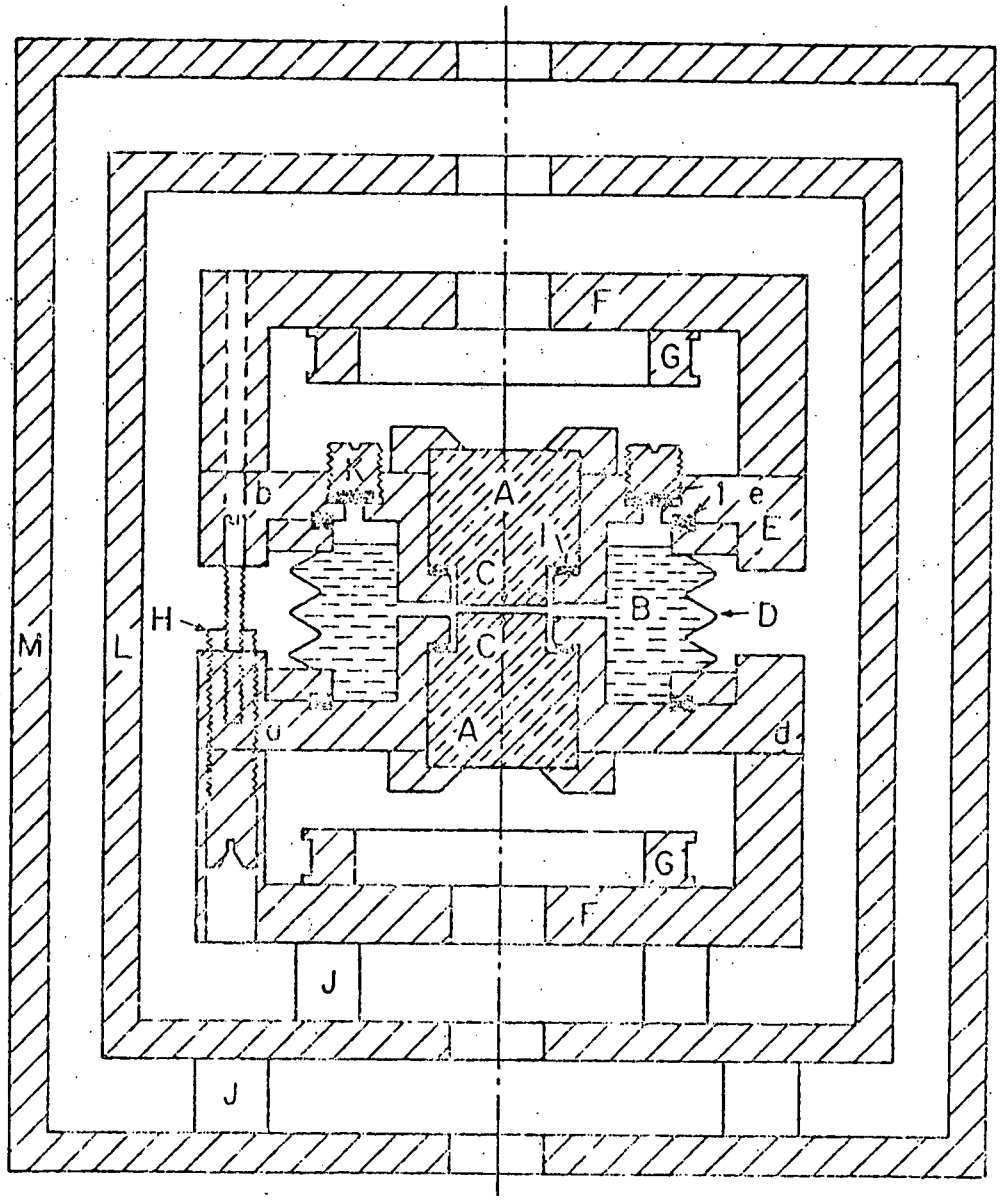

Fig. 2. Experimental Cell. Diagram of experimental cell inside its heat shield and vacuum container with A: quartz optical flats; B: fluid reservoir; C: high reflectivity coatings; D: stainless steel bellows; E: stainless steel cell half; F: aluminum end caps; G: heaters; H: invar differential screw (one of three); I: teflon seals; J: nylon support posts; K: fill port; L: heat shield; M: vacuum container; and a,b,d,e,: locations of thermistors.

flats showed more curvature, and a flatness of approximately $\lambda/30$. The original flats used in the experiment were coated with a multilayer dielectric coating peaked for high reflectivity at 6328 Å. Exposure to the 2,6-lutidine + water mixture resulted in rapid deterioration of the coatings, and so the flats were recoated with a dielectric coating protected by a one wavelength thickness of SiO_2. This 0.425 μm overcoat of SiO_2 on each surface had an index of refraction of 1.49 (in contrast with 1.46 for bulk fused silica). These coatings and a subsequent similar coating were used for approximately two months before significant deterioration occurred. The flats were then recoated with silver and additional data were taken for six months before substantial damage to the coatings occurred. Data taken before, during, and after deterioration of the coatings had the same critical temperatures and coexistence curves.

The laser used to illuminate the flats was a 1/2 mW He-Ne laser. After passing through a beam expander the intensity of the light was adjusted by using neutral density filters. The traveling telescope used to measure fringe positions was precise to ±1 μm.

2.2 Temperature control

The cell temperature was controlled with an AC bridge using a YSI 44004 thermistor as the sensing element. The thermistor was mounted at position a in Fig. 2. The cell temperature could be controlled to ±0.1 mK for periods of several days. The heat shield surrounding the cell was controlled by a DC bridge and rate sensing power amplifier using another YSI 44004 thermistor as the sensing

element. The heat shield could be controlled to ±1 mK for periods of several days.

The cell temperature was monitored using a separate AC bridge that has been described elsewhere (Lyons, Mockler, and O'Sullivan, 1974), and three YSI 44004 monitor thermistors located at b, e, and d in Fig. 2. The thermistor located at b had been previously calibrated with an NBS calibrated Standard Platinum Resistance Thermometer to give an accuracy of ±10 mK in our absolute temperature determinations. The temperatures used in our analysis were those measured with this thermistor. The three monitor thermistors were used as a set to determine the cell temperature stability and the stability against drift of the thermistors themselves. Intercomparisons made over a period of several weeks within a temperature range of one degree showed discrepancies among these thermistors of less than 1 mK. These variations were due to errors in cross-calibration and small changes of thermistor resistance with time. To check for long term drift in the thermistors, critical temperature measurements at certain spacings were repeated after several months. These measurements showed no systematic long term drift within the measurement uncertainty.

The shield temperature always "tracked" the cell temperature with a -100 mK difference. This served to minimize gradients and insure that any gradients present would not change with time or cell temperature. Comparison of the monitor thermistors at e and d in Fig. 2 and adjustment of the heaters in the cell end caps allowed us to trim the temperature gradient between e and d to less

than 1 mK. At large spacings all of the fringes in the field of view should go through the critical point simultaneously if all portions of the fluid between the flats have the same temperature and critical concentrations. Any radial gradient across the flats would cause some fringes to go through the transition before others. No such systematic dependence of apparent critical temperature upon position was observed.

At one point during the course of these experiments the entire apparatus was disassembled and moved to another laboratory. This move occurred just after the experiments with the multi-dielectric coated flats were completed. The apparatus was reassembled and some minor changes and adjustments were made. Intercomparisons of the various monitor and control thermistors showed variations of up to 10 mK from the previous values. These changes led to more uncertainty in subsequent absolute temperature measurements. All thermistors continued to agree, however, as to the magnitude of temperature changes.

2.3 Fluids

The 2,6-lutidine + water mixture was chosen for use in these experiments for a variety of reasons. The mixture has a critical temperature of 34 C which is easily accessible. The large index of refraction mismatch between the two components (the index of refraction of water is 1.33, while the index of refraction of lutidine is 1.50) leads to comparatively large index of refraction differences between the two phases. Consequently, index of refraction difference

measurements are a sensitive measure of the relative concentrations in the two-phase region. In other systems, such as methanol + cyclohexane, contamination by water is a serious problem, which can lead to large shifts in the critical temperature (Jones and Amstell, 1930). Since water is one component of our mixture it cannot cause problems as an impurity, tending only to introduce minor offloading effects. Finally, the fact that we are studying the lower critical point of lutidine + water leads to greater ease of preparation. The system is in the one-phase region at room temperature and so one large sample of the fluids with the critical concentration can be mixed and stored at room temperature. Numerous small chemically identical samples can be drawn off from this stock solution for various experiments. Four samples were drawn off from the stock solution over a period of four months. All had critical temperatures at large spacings within 2 mK of each other. Thus when the cell required recharging because of optical coating failure we were assured that the cell could be reloaded with an identical sample.

The 2,6-lutidine used in the experiment was obtained 99% pure from Eastman Kodak Company. It was further purified for the critical mixture by distillation in a nitrogen atmosphere. The water used was triply distilled and deionized. 300 cm^3 of the critical mixture were mixed with a concentration of 28.702% by weight lutidine (Loven and Rice, 1963). This 300 cm^3 formed the stock solution that was drawn on as needed throughout the experiment. The bulk critical temperature of the mixture was 33.98°C. Other values for the critical temperature quoted in the literature range from 33.57 C

(Gutschick and Pings, 1971) to 34.06 C (Cox and Herrington, 1956).

Each loading of the cell required approximately 45 cm^3 of the critical mixture. The cell was massed just before and after three data runs to check for leakage of the fluids. These measurements indicated that the fluid loss was less than 0.02% of the original fluid mass after periods of two to four weeks.

CHAPTER III

EXPERIMENTAL PROCEDURE

3.1 Film Preparation

The following procedure was used to insure that the fluid in the film between the flats was homogeneous in concentration and that it had the same concentration as the bulk fluid in the cell volume surrounding the flats. The cell was first removed from its temperature controlled environment and allowed to cool to room temperature, approximately 11 C below the critical temperature in the one-phase region. The flats were then brought together to within a few microns, squeezing the fluid between them out into the reservoir. The cell was then vigorously shaken to mix the fluids in the reservoir. The cell was left at room temperature and after several hours of equilibration the flats were pulled ~300 μm apart, drawing in a homogeneous mixture from the reservoir. After several more hours the flats were brought together again, expelling the sample. This procedure was repeated several times over two to four days before reinserting the cell into the heat shield and vacuum can.

We were forced to adopt the above technique because of lack of reproducibility of critical temperatures and coexistence curves in early data runs where a less careful preparation procedure was used. When the temperature of a sample goes through the critical temperature into the two-phase region phase separation occurs and

concentration inhomogeneities appear between the flats. If the temperature is then dropped back below the critical temperature into the one-phase region these inhomogeneities can persist for long periods of time. The sample preparation technique we used in the early work did not insure that subsequent samples had a homogeneous critical concentration. Thus, lack of reproducibility in the concentration of the fluids between the flats led to large scatter in our data. The lengthier preparation technique has resulted in much improved reproducibility of our $T_c(L)$ measurements. However, much of the remaining scatter in the data is no doubt due to this problem of exactly reproducing the critical concentrations of the fluids in our trapped samples.

After preparation of a sample as described above, the cell was heated to 0.5 C below the critical temperature (in the one-phase region) and the spacing between the flats was measured and adjusted. Standard optical coincidence techniques were used with a variety of light sources to measure the spacing between the flats. For the silver coated flats fringes form at points on the flats where

$$L = \frac{m\lambda_o}{2n} \quad . \tag{3.1}$$

Here L is the spacing between the flats, the integer m labels the fringe order, λ_o is the vacuum wavelength of the light source used, and n is the index of refraction of the fluid mixture. We use $n = 1.385$, the value determined using a prism cell for the index of refraction of our mixture at $\lambda_o = 6328$ Å and at T_c (Handschy, 1978). Different sources with different vacuum wavelengths will

produce fringes at different points on the flats according to the above relation. Measurements of the positions of the fringes formed with these different sources allow us to calculate the spacing at various points between the flats. These spacing measurements have typical uncertainties of 3%, due to uncertainties in position measurements, dispersion, and temperature dependence of the index of refraction. For the silver coated flats the fluid film thickness is the spacing between the flats. For the dielectric coated flats the above procedure gives the spacing between the reflective coatings of the flats to a close approximation. To obtain the film thickness the thickness of the protective SiO_2 overcoats must be subtracted off.

3.2 Finding T_c

Following adjustment of the spacing to the desired value, the cell temperature was raised to typically 20 mK below the critical temperature. The system was then allowed to equilibrate for one or two days, after which the spacing was rechecked and the temperature slowly raised to find $T_c(L)$. Typically the temperature was changed in 1 to 2 mK steps separated in time by 2 or more hours.

For all spacings the fringes become dim and granular in appearance as the critical point is approached. There are other features of the fringes at the critical point that depend upon the spacing, however. For spacings larger than approximately 50 μm the fringes disappear at some point as the temperature is raised. They are replaced by a "milky way." That is, numerous bright points of light imbedded in a background glow fill the field of view in the

telescope. If the temperature is left unchanged, very serpentine fringes, indicating large concentration gradients will appear within an hour. These fringes will gradually straighten out and a clear meniscus will form if the system is left undisturbed for a day. Thus, for the larger spacings, we identify the critical temperature as lying between the temperature where the fringes disappear and the last temperature where the fringes were present.

For spacings less than 10 μm the fringes do not disappear but instead split at some temperature. If the temperature is further increased the splitting increases and is measured as a function of temperature. T_c is ultimately determined by fitting the resulting coexistence curve data and extrapolating back to the point of zero splitting (see Chap. IV for details).

For intermediate spacings of 10 to 50 μm the fringes disappear at the critical temperature, as at the larger spacings. However, they reappear within 1/2 hour as split fringes. If the temperature is then raised further the splitting increases and can be measured as a function of temperature, thus providing coexistence curve data. Extrapolation of these measurements back to the point of zero splitting gives values for the critical temperatures which agree within our experimental precision with those determined from observation of the fringe disappearance.

As mentioned above, temperature steps of 1 to 2 mK were used in raising the temperature of the cell to locate $T_c(L)$. Although we would have been able to locate T_c more precisely by taking smaller temperature jumps, we were forced to take such sizable

steps because of the following. For the silver coated flats the critical temperature of the fluid film between the flats is higher than the critical temperature of the bulk fluid in the reservoir. Thus, as we raise the temperature to find T_c for the film, the fluid in the reservoir goes through the transition before the fluid between the flats. As soon as the fluid in the reservoir goes through the transition the two bulk phases begin to leak in between the flats, displacing the critical mixture there. This is seen as curvature of the fringes around the edges of the flats. Thus we were forced to take 1 to 2 mK temperature jumps in order to raise the temperature rapidly enough to find $T_c(L)$ for the film before the fluid concentration in the central region of the flats was altered. At spacings less than 10 μm no leakage could be seen for periods of up to a week. However, at a spacing of 100 μm the leakage is much more rapid and completely alters the concentration between the flats within 12 hours.

The time allowed for equilibration of the fluid films between temperature changes was approximately 2 hours. We feel that this was a sufficient equilibration time for three reasons. First, when phase separation occurs in our films it almost always occurs within a few minutes of a temperature change. This indicates that the fluid films react to temperature changes within a few minutes. Second, when the temperature is changed the fringes move because the index of refraction of the fluids is temperature dependent. In the one-phase region measurements of fringe positions showed that after a temperature change on the order of 1 mK the fringes

moved to their new positions within a few minutes. This again indicates that the films react very quickly to temperature changes. Finally, a large collection of fringe splitting measurements as a function of temperature were broken into two groups. One group consisted of data taken 3 or more hours after the last temperature change. The other group consisted of data where the equilibration times were from one to three hours. No systematic difference could be found between the two groups. All of the above indicate that the fluids between the flats equilibrate very quickly after temperature changes and that 2 hours is sufficient equilibration time.

There are several factors which promote this rapid equilibration after temperature changes. The flats and the coatings are heated directly by radiation from the heater coils. Since the fluid under study is a film lying between these surfaces, the thermal equilibration of the fluid is a rapid process. In the two-phase region we have drops of one phase surrounded by portions of the other phase. After a temperature change the concentrations of lutidine and water in the two phases change to new values. This readjustment proceeds by diffusion. Since the drops are typically a few hundred microns in diameter this diffusion process occurs quite rapidly.

3.3 Measurement of Δn

At the smaller film thicknesses where the fringes split, careful measurements of the fringe splitting as a function of temperature were made. These measurements allowed us to calculate Δn, the index of refraction difference between the two phases of

the fluid, which can ultimately be related to the concentration difference between the two phases.

Figure 3 is a diagram of the region between the silver coated flats at a temperature and spacing where split fringes are observed. A is a drop of the water-rich phase surrounded by B, the lutidine-rich phase. Fringes have formed at points p_1, p_2, p_3, and p_4. Since fringes form at points where the film thickness, L, is an integral number of half wavelengths, the spacings at p_1, p_2 and p_3 must satisfy Eq. (3.1). Thus

$$L_1 = m_B\lambda_o/2n_B \quad , \quad L_2 = m_A\lambda_o/2n_A \quad \text{and} \quad L_3 = (m_B+1)\lambda_o/2n_B$$

where n_A and n_B are the indexes of refractions of the two phases and $n_A < n_B$. If $n_B - n_A \equiv \Delta n$ is small (in all of our data $\Delta n < 0.04$) and if the spacing is small, then $m_A = m_B = m$, which is known from the spacing measurements. If ϕ is the wedge angle of the flats then $\tan \phi = (L_3-L_1)/x = (L_2-L_1)/y$, where $x = p_3 - p_1$ and $y = p_2 - p_1$. Setting $(n_A+n_B)/2 = n$ and assuming $\Delta n << n$ the above expressions can be combined to give

$$\Delta n = (ny)/(mx) \quad . \qquad (3.2)$$

Thus, if the spacing and the average index of refraction are known, measurements of fringe splittings can be converted to differences in index of refraction between the two phases.

Several additional points need to be made about the above development. In Fig. 3 the choice of $x = p_3 - p_1$ is not unique. For example, x can be chosen as p_4-p_2 and the analysis will give the same results for Δn. In actual practice fringes to the left

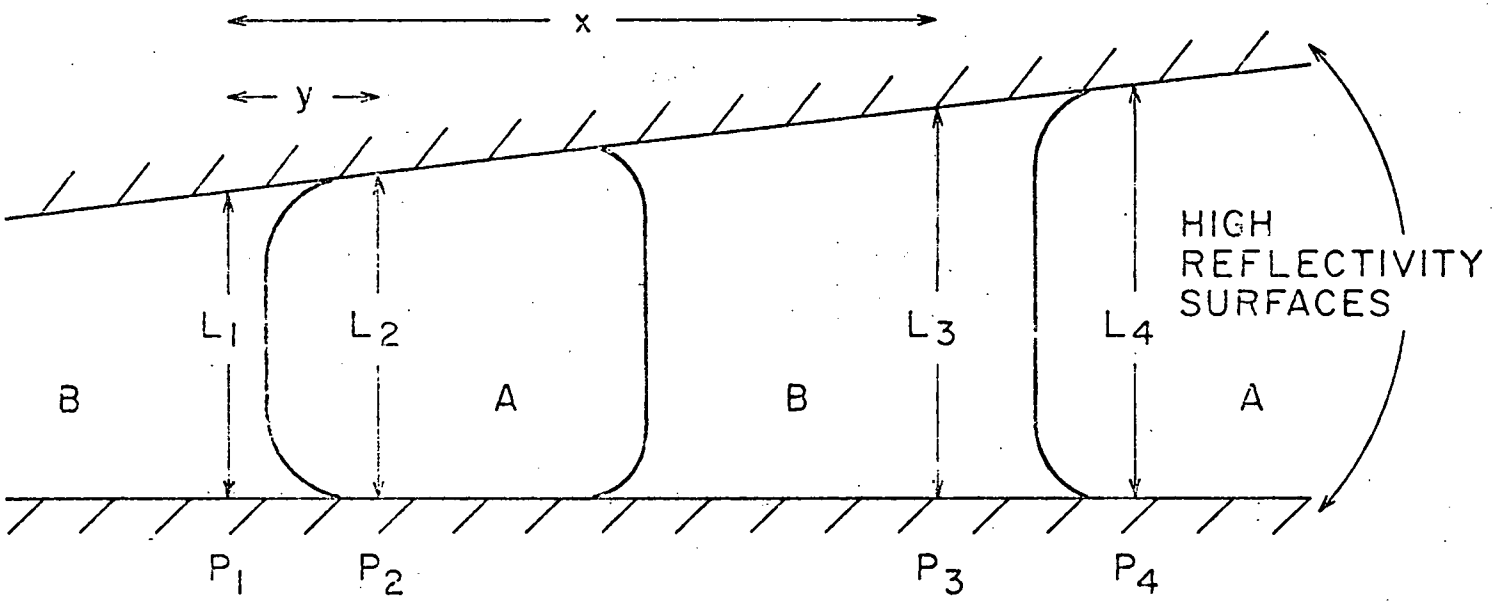

Fig. 3. A wedge of fluid trapped between the optically flat surfaces.

of p_1, as well as fringes to the right of p_2 were used to determine x. This averaging of x values led to better statistics and compensated to first order for curvature of the flats.

It can be seen from Eq. (3.2) that the splitting, y, is proportional to x. Since the largest source of error in the calculations of Δn is the measurement of y we would like to have large x values in order to increase our sensitivity. However, as x is increased the number of fringes in the field of view decreases. We have compromised by adjusting the wedge angle so that 3 to 5 pairs of fringes were in the field of view. This gave adequate sensitivity while allowing us to take data simultaneously at 3 to 5 film thicknesses.

It can be seen from Eq. (3.2) that since m is proportional to L the sensitivity of our Δn measurements is proportional to the film thickness. Thus at a 0.45 μm spacing we have one tenth the sensitivity that we have at 4.5 μm.

In all of the calculations of Δn we have used $n = 1.385$, the value for the refractive index at the critical temperature referred to previously. Measurements of n_A and n_B for bulk samples have been made using a prism spectrometer (Handschy, 1978). From these measurements we find that $n \equiv (n_A + n_B)/2$ changes less than 0.06% per deg K near the critical point. Since our measurements have all been made within 1.5 C of T_c, the change in n over the range of our measurements was less than 0.1%. This effect was ignored in the analysis since it is an order of magnitude less than the typical uncertainties introduced by the fringe position measurements.

Ideally, we would have liked to measure n_A and n_B separately in the films rather than their difference, Δn. This was impractical in our cell due to a constant drift in the spacing. Mechanical relaxations in the cell caused the spacing between the flats to change ~10 Å per hour. This led to a drift in fringe position of typically 15 μm per hour. For an absolute determination of the refractive indexes this drift would have to be taken into account. However, it has practically no effect upon our measurements of refractive index differences.

Measurements of the positions of the split fringes had typical standard deviations of 5 μm. In the early experiments, fringe positions were measured at only the midpoint of each fringe along its length. In later experiments fringe splittings were measured at a variety of points on each set of split fringes. These splitting measurements showed larger scatter than expected. In part this scatter was due to the drops forming the split fringes. That is, when a fringe passes through the edge of a drop it becomes smeared out and difficult to measure. These variations in splitting did not depend on equilibration time or position on the flat. This enhanced scatter may indicate a small dependence of index of refraction upon drop size.

In order to be able to estimate the uncertainties in the measurements of the fringe splittings, y, we made multiple measurements of the splitting at a number of y values. These measurements were then used to find the behavior of the standard deviation of the fringe splitting measurements as a function of y.

From this analysis we found that the uncertainty, σ_y, in a given measurement of y, could be estimated using $\sigma_y = \pm(12\ \mu m \pm 0.005\ y)$ with y in microns. This form for the uncertainty in y was used in determining the error bars on the Δn measurements.

CHAPTER IV

COEXISTENCE CURVE ANALYSIS

4.1 Lorentz-Lorenz relation

The Lorentz-Lorenz equation relates the index of refraction of a mixture to the mass fractions of its separate components. If the volume of the mixture is equal to the sum of the volumes of the separate components before mixing then this equation allows one to relate the index of refraction of the mixture to the volume fractions of the separate components. In the two phase region of a binary fluid mixture this application of the Lorentz-Lorenz relation yields the result $\Delta\phi \equiv \phi_1 - \phi_2 = K(n_1 - n_2)$ (see Jacobs et al., 1977). ϕ_1 is the volume fraction of one of the components in phase 1, and ϕ_2 is the volume fraction of the same component in phase 2. n_1 and n_2 are the indexes of refraction of phases 1 and 2, respectively. Over the 1.5 C range of temperatures within which all our data fall, K changes less than 0.03% and so will be treated as a constant. Thus in analyzing our data we can consider $\Delta n = n_1 - n_2$ proportional to $\Delta\phi$. We take $\Delta\phi$ as the order parameter of the system (Stein and Allen, 1973) and so its behavior is governed by the coexistence curve scaling form

$$\Delta\phi = A^* \left[\frac{T - T_c}{T_c}\right]^{\beta} , \qquad (4.1)$$

where A^* is a constant and β is the critical exponent. The near proportionality of Δn and $\Delta\phi$ then implies that Δn also maps out the coexistence curve and we shall write

$$\Delta n = A \left[\frac{T - T_c}{T_c} \right]^{\beta} \quad . \tag{4.2}$$

This form for the relation between Δn and $T - T_c$ in a binary fluid mixture has been tested experimentally by Jacobs et al. (1977). They measured Δn in a bulk sample of methanol + cyclohexane and found that Eq. (4.2) provided a good fit to their data with a value for the critical exponent of $\beta = 0.326$. This value agrees well with other experimental values and with recent theoretical estimates (Stanley, 1971 and Guillou and Zinn-Justin, 1977). Thus we expect the Δn vs. T measurements to map out the coexistence curve of our system for a variety of film thicknesses.

4.2 Qualitative discussion of the data

When we plot the data for Δn vs. T we do not see the smooth curve expected from Eq. (4.2). Instead an extra tip appears to be added onto an apparently normal coexistence curve. Figure 4 is a plot of a typical set of data. The solid lines are the results of fits to the data and will be discussed later. It is apparent in Fig. 4 that in the region labeled A the behavior of the system is changing. We call such a region the crossover region. Although this behavior in one set of data might be dismissed as due to unusual scatter, we have observed such tips and accompanying cross-over regions in each of 32 data sets where the film thickness was

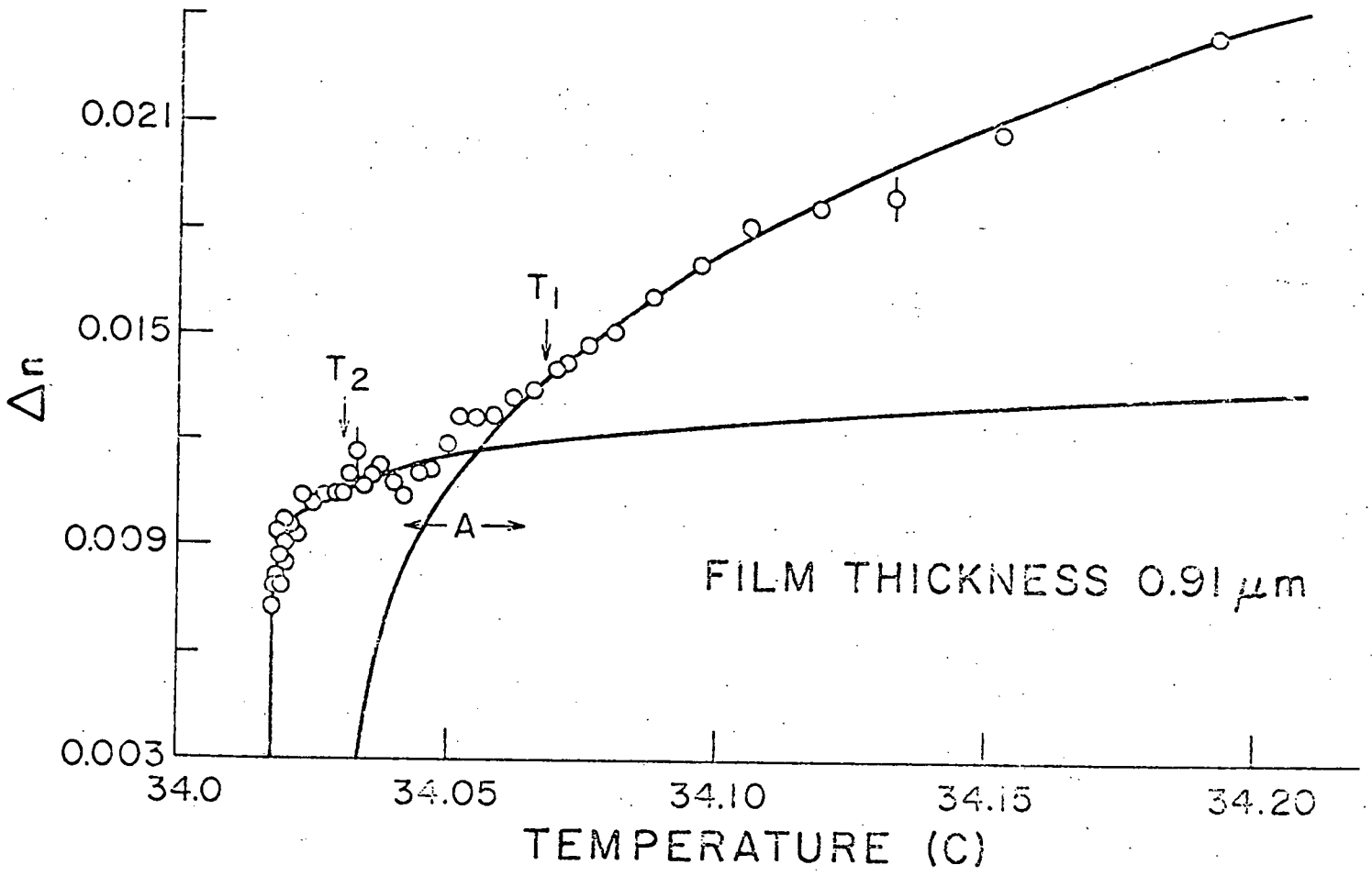

Fig. 4. Typical Δn versus temperature measurements.

less than 6 μm. To analyze this behavior we treated the data above and below the crossovers separately. For film thicknesses where fringe splitting occurred Eq. (4.2) was fit to the data above the crossover. The average value of β from these fits was 0.335. We interpret this to mean that the coexistence curve segments above the crossover display normal three dimensional behavior. When Eq. (4.2) is fit to the data below the crossovers the unweighted average value of β is 0.132. The 2d Ising model predicts a coexistence curve of the same form as Eq. (4.2) with $\beta = 0.125$. This suggests that below the crossover region we are observing two dimensional scaling behavior, where the crossovers demarcate two distinct scaling regimes.

We will refer to $T - T_c$ values below the crossovers on plots such as Fig. 4 as lying in 2d regions, and values above the crossovers as 3d regions. Parameters obtained by fitting Eq. (4.2) to data in the 2d region will be denoted by A_2, β_2, T_{c2}. Parameters obtained by fitting to data in the 3d region will be denoted as A_3, β_3, T_{c3}.

4.3 Details of fitting procedure

In order to find A_3, β_3, and T_{c3} for a given data set we plot the data as in Fig. 4. To find the best values for the parameters we fit Eq. (4.2) to all 3d data in the set without including any data from the crossover region. It is difficult from inspecting such a plot, however, to determine exactly where the 3d region ends and the crossover region begins. Confronted with this difficulty

we were forced to make a number of fits to the data, assuming different values for the crossover temperature in each fit. Examination of the results of these fits allowed us to determine the best values for the parameters.

The fitting procedure began by examining the plot of the data to roughly locate the crossover region and to estimate T_{c3}. T_{c3} was estimated by a smooth curve extrapolation of the 3d data to $\Delta n = 0$. We then picked a temperature, T_1, lying clearly in the 3d region (see Fig. 4 for example) and fit Eq. (4.2) to the subset of the data with $T \geq T_1$. [The fit actually was made using $\Delta n = A' (T - T_c)^{\beta}$, where $A' = A/T_c^{\beta}$.] This fit began by using the estimated value for T_{c3} in a weighted grid search to find starting values for A_3' and β_3. The weighting factors were determined using the error bars on the Δn measurements and the estimated uncertainty in $(T - T_c)$. In this coarse grid search the reduced χ^2 was calculated for each of 240 pairs of values for β_3 and A_3' (test values for β_3 ranged from 0.07 to 0.39). The pair of values for β_3 and A_3' resulting in the smallest χ^2 was then used with the estimated T_{c3} as starting values for GRIDLS (Bevington, 1969), a weighted fitting routine, which returned improved values for A_3', β_3 and T_{c3}, associated relative uncertainties, and a new reduced χ^2. If GRIDLS had reduced the χ^2 by more than 1% the data subset was refit using the improved values of A_3, β_3, and T_{c3} as the starting points. GRIDLS was used repeatedly in this way until the χ^2 values for successive fits differed by less than 1%. The values of A_3, β_3, T_{c3} and their uncertainties as well as the χ^2 from this last fit to the subset were tabulated and A_3 was calculated using A_3', β_3 and T_{c3}.

We then expanded this 3d data subset by adding the highest temperature datum not previously included and fit Eq. (4.2) to this expanded subset. This fit used the results for the parameters from the previous fit as starting values and began directly with GRIDLS, omitting the coarse grid search. As before, GRIDLS was used repeatedly until it improved the χ^2 of the fit by less than 1%. After noting the final results of this fit another point was added to the 3d region. This new 3d subset was then fit as before, omitting the coarse grid search again.

We continued in this way adding points one at a time to the 3d region and fitting Eq. (4.2) to each new 3d set until we reached a temperature T_2 clearly in the 2d region (see Fig. 4). As the points were added to the 3d region, slowly enlarging it, the reduced χ^2 and A_3', β_3, and T_{c3} determined from the successive fits were relatively constant until points in the crossover region were included. As points in the crossover region were included the reduced χ^2 began to monotonically increase and the values of the parameters began to change systematically. Examining the results of the above fits, we then chose as our best values for the A_3', A_3, β_3 and T_{c3} the values obtained from the fit that gave the smallest reduced χ^2. The above procedure was followed for each of 30 data sets taken with the silver coated flats where sufficient 3d data was available.

To find A_2, β_2 and T_{c2} for each data set we followed a procedure similar to that described above for the 3d parameters. We began by fitting Eq. (4.2) to the data in each set with $T \leq T_2$, with T_2

clearly in the 2d region. We then added to this 2d set the lowest temperature point not previously included and refit the data. We continued adding points of higher temperature, enlarging the 2d region, and fitting each new set until we reached T_1. The behavior of the fits as more points were included was similar to that in the 3d region. That is, the values of the reduced χ^2 and the parameters changed little until points in the crossover region were included, whereupon systematic changes began to appear. Again, we chose as the best estimates of the parameters those obtained from the fit with the smallest reduced χ^2. The same fitting routines were used for these 2d data as for the 3d data with two modifications. First, T_{c2} was constrained to temperatures less than the temperature of the lowest temperature datum point. Second, the initial starting value for T_{c2} was chosen for each set to be 0.2 mK lower than the temperature of the lowest temperature data point in the set. 27 sets of data taken with the silver coated flats were fit in this way to find 2d values for the parameters. Three other sets of data at spacings of approximately 14 μm showed no 2d region, and so could not be fit this way.

Having determined the 2d and 3d parameters by the above procedures we plotted the resulting 2d and 3d coexistence curves with the data for each set. The solid lines in Fig. 4 are the 2d and 3d coexistence curves for that data set. By examining these plots and the calculated residuals we checked the quality of the fits. In some cases the data were then refit using different starting values for T_1, T_2 and T_{c3} resulting in improved fits.

As stated above, 30 sets of Δn vs. T measurements were analyzed in this way. They covered a range of film thicknesses from 0.46 μm to 14.9 μm. The average data set had 40 points with typically a third of these points in the 2d region. The original fits of the 30 data sets showed a total of approximately 20 points which lay more than 3σ away from the fitted curves. These points were then eliminated from subsequent fits. The Δn versus T data for the silver coated surfaces are tabulated in the Appendix.

CHAPTER V

RESULTS

5.1 Coexistence curves

In the previous section we discussed the method of analysis used to treat the data. In this section we present the results of that analysis. Since most of the data were taken with silver coatings on the flats, we first discuss those results.

Figure 5 is a plot of the values for the critical exponent β_3 found by fitting to the 3d region for 30 data sets. The dashed line is the average value. There is no apparent dependence of β_3 upon film thickness and further investigation reveals no systematic dependence of β_3 upon either the position of the fringes on the flat or upon whether the data were taken in an earlier or later run. The average value of β_3 is 0.335 ± 0.003. The quoted uncertainties in all determined parameters will be one standard deviation values. The weighted average using the relative uncertainties obtained from the fits as the weighting factors is $\beta_3 = 0.332 \pm 0.003$.

Figure 6 displays the values for the coefficient A_3 of the coexistence curve found by fitting the 3d data. The average value is $A_3 = 0.321 \pm 0.005$, while the weighted average is $A_3 = 0.311 \pm 0.005$. The dashed line in Fig. 6 is the average value. Within the precision of our measurements A_3 appears to be independent of spacing, position of the fringes or time. Using Lorentz-Lorenz as discussed

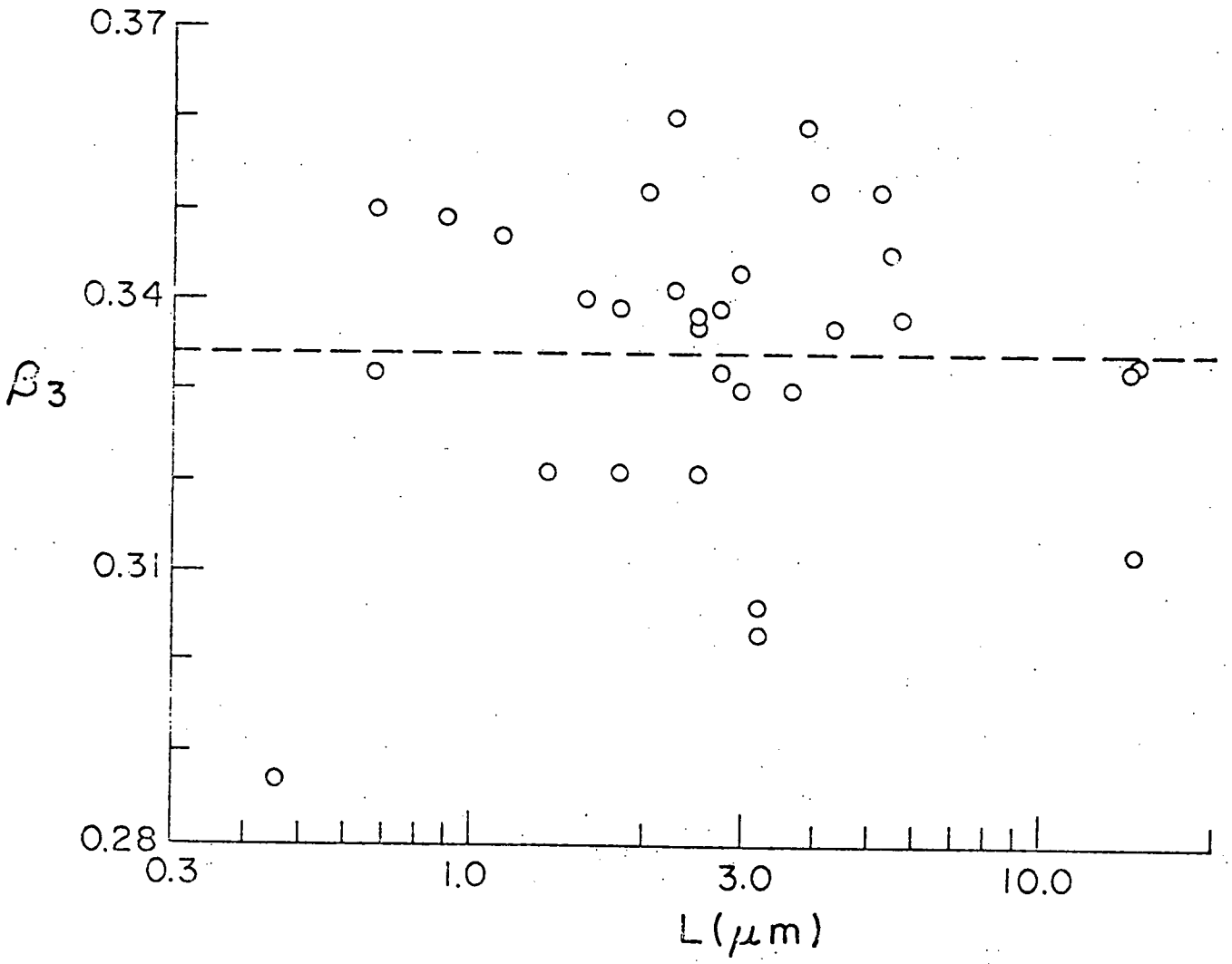

Fig. 5. Critical exponent β_3 versus film thickness.

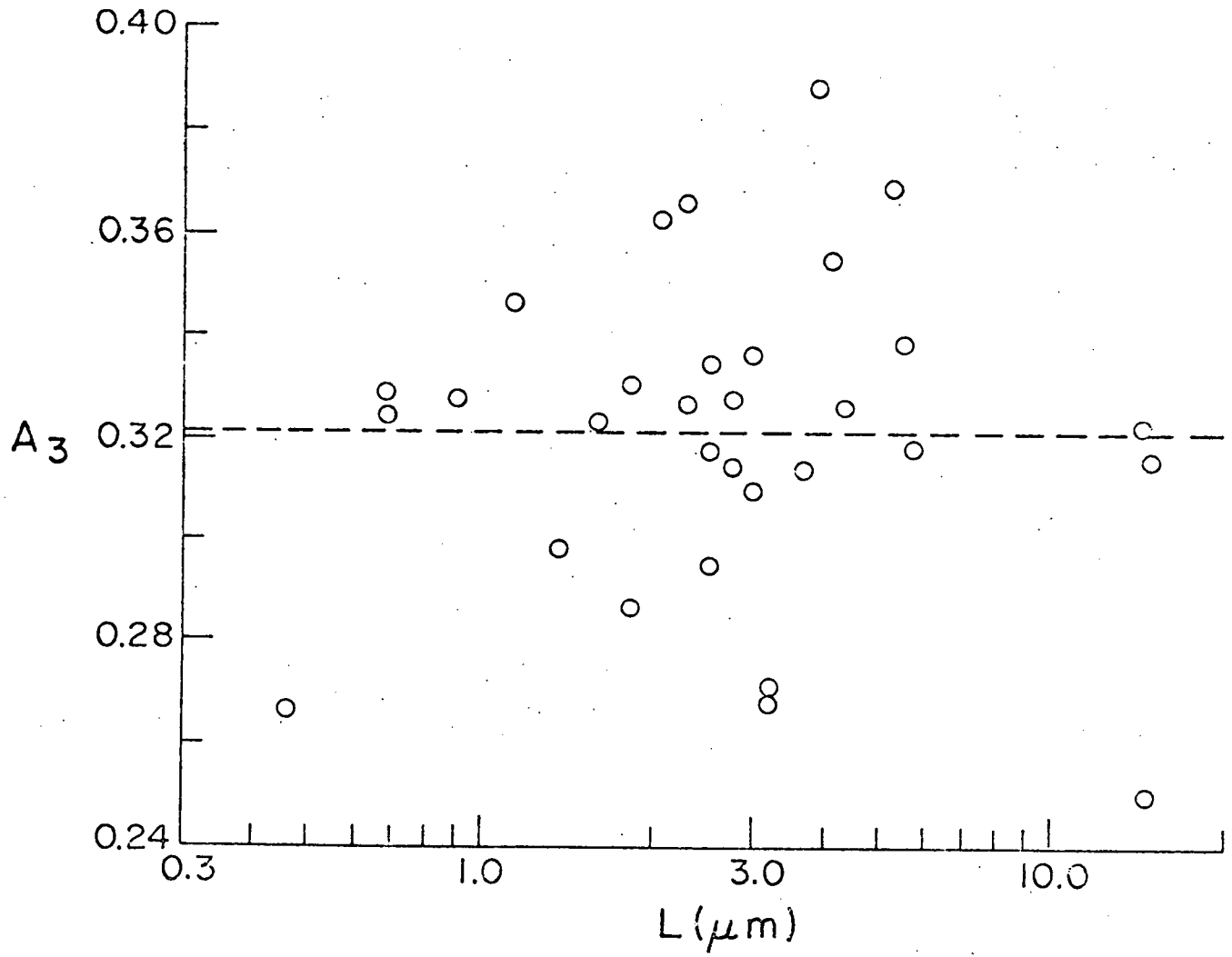

Fig. 6. Coexistence curve coefficient A_3 versus film thickness.

before we can use the average value of A_3 to calculate A^*, [$\Delta\phi = A^*\epsilon^{\beta}$, $\epsilon = (T - T_c)/T_c$], and find $A^* = 1.91 \pm 0.03$. Stein and Allen (1973) have fit the bulk lutidine+water coexistence curve data of Loven and Rice (1963) and found $A^* = 1.95 \pm 0.70$. Thus our value for A^* and hence A_3 appears to be reasonable.

The importance of the above results is that they support the contention that our Δn vs. T measurements map out the coexistence curve of the system. For each data set $\Delta n = A_3\epsilon^{\beta_3}$, $\epsilon = \{[T - T_{c3}(L)]/T_{c3}(L)\}$, provides a good description of the 3d data. The 30 values found for β_3 and A_3 are presented in Table I.

Figure 7 contains the values for β_2 obtained by analyzing 27 sets of 2d data. The dashed line is the average value. We find no systematic variation in the values. There is more scatter in the 2d values than in the 3d values, probably because there are less 2d data in each run and the data cover a more limited $T - T_c$ range. The average value of β_2 is found to be 0.132 ± 0.007, while the weighted average is 0.126 ± 0.005. These values are very close to the 2d Ising model value of 0.125, a result which strongly suggests that, over a limited $T - T_c$ range about the critical point, our fluid films are behaving as 2d Ising systems. The 27 values found for β_2 are presented in Table II.

Figure 8 is a plot of the coefficients A_2 found by fitting the data sets. The numerical values are listed in Table II. The average value of A_2 is 0.035 ± 0.002 (the dashed line in Fig. 8) while the weighted average is $A_2 = 0.028 \pm 0.002$. Surprisingly, the average value and the weighted average are significantly different. Although

TABLE I

Values for β_3 and A_3 found for data taken with silver coated surfaces

Data Run	Film Thickness (μm)	β_3	A_3
1	2.28	0.341	0.326
1	2.51	0.338	0.335
1	2.74	0.339	0.328
1	2.97	0.343	0.337
1	3.20	0.306	0.271
2	2.51	0.321	0.295
2	2.74	0.332	0.315
2	2.97	0.330	0.310
2	3.20	0.303	0.268
3	1.83	0.339	0.330
3	2.06	0.352	0.363
3	2.28	0.360	0.366
3	2.51	0.337	0.318
3	2.74	0.332	0.314
4	0.69	0.322	0.329
4	0.91	0.349	0.328
4	1.14	0.347	0.347
5	5.25	0.352	0.369
5	5.48	0.345	0.339
5	5.71	0.338	0.318
6	14.39	0.332	0.322
6	14.62	0.312	0.250
6	14.85	0.333	0.316
7	1.37	0.321	0.299
7	1.60	0.340	0.323
7	1.83	0.321	0.287
8	3.66	0.330	0.314
8	3.88	0.359	0.388
8	4.11	0.352	0.355
8	4.34	0.337	0.326
9	0.46	0.287	0.267
9	0.69	0.350	0.324

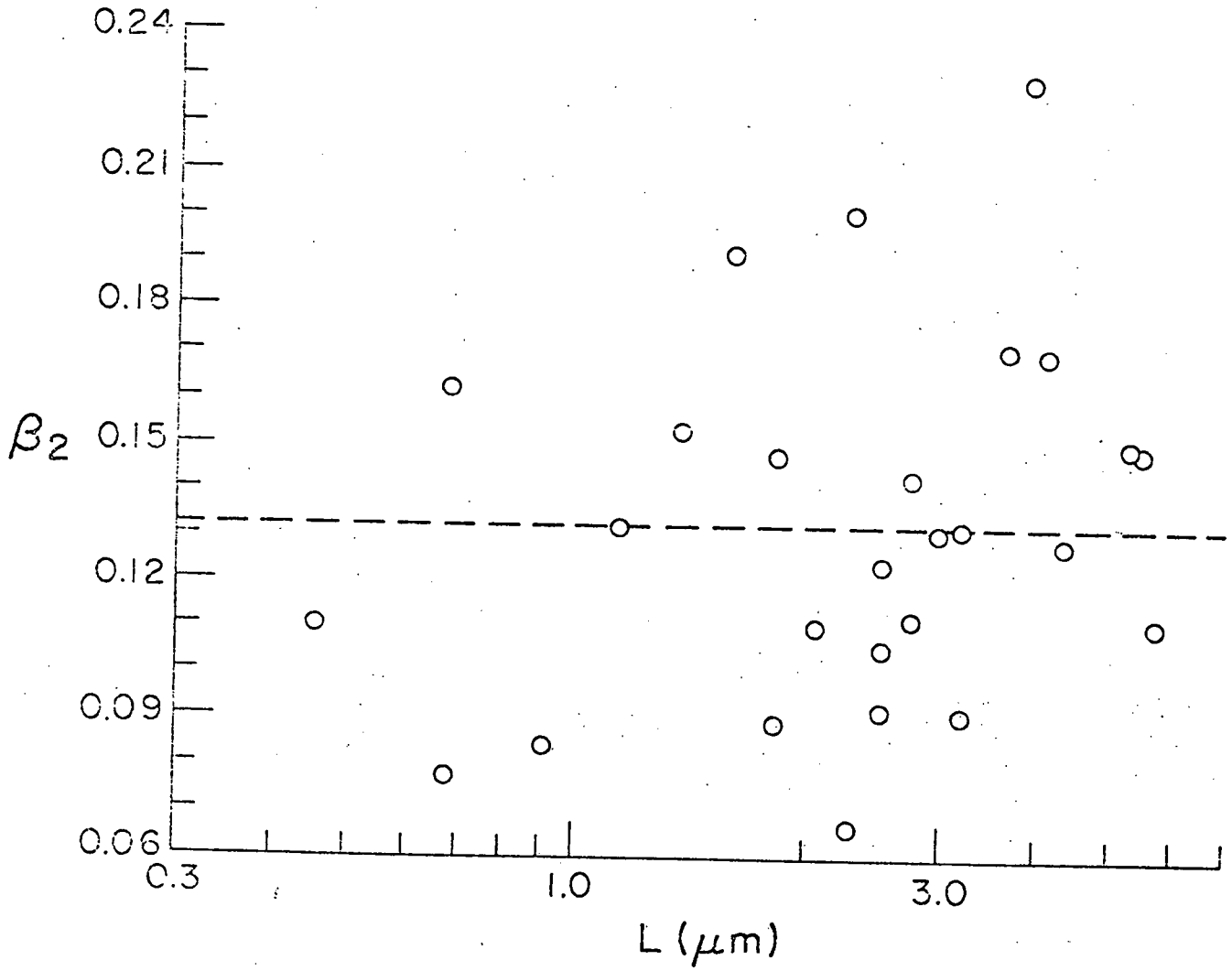

Fig. 7. Critical exponent β_2 versus film thickness.

TABLE II

Values for β_2 and A_2 found for data taken with silver coated surfaces

Data Run	Film Thickness (μm)	β_2	A_2
1	2.28	0.201	0.0680
1	2.51	0.092	0.0190
1	2.74	0.143	0.0365
1	2.97	0.131	0.0303
1	3.20	0.132	0.0366
2	2.51	0.124	0.0370
2	2.74	0.112	0.0329
2	2.97	0.131	0.0419
2	3.20	0.091	0.0327
3	1.83	0.089	0.0236
3	2.06	0.110	0.0257
3	2.28	0.067	0.0151
3	2.51	0.105	0.0255
4	0.69	0.077	0.0267
4	0.91	0.084	0.0248
4	1.14	0.132	0.0366
5	5.25	0.150	0.0335
5	5.48	0.149	0.0333
5	5.71	0.111	0.0213
7	1.37	0.153	0.0437
7	1.60	0.192	0.0511
7	1.83	0.148	0.0350
8	3.66	0.171	0.0383
8	3.88	0.230	0.0635
8	4.11	0.170	0.0297
8	4.34	0.129	0.0230
9	0.46	0.110	0.0471
9	0.69	0.162	0.0526

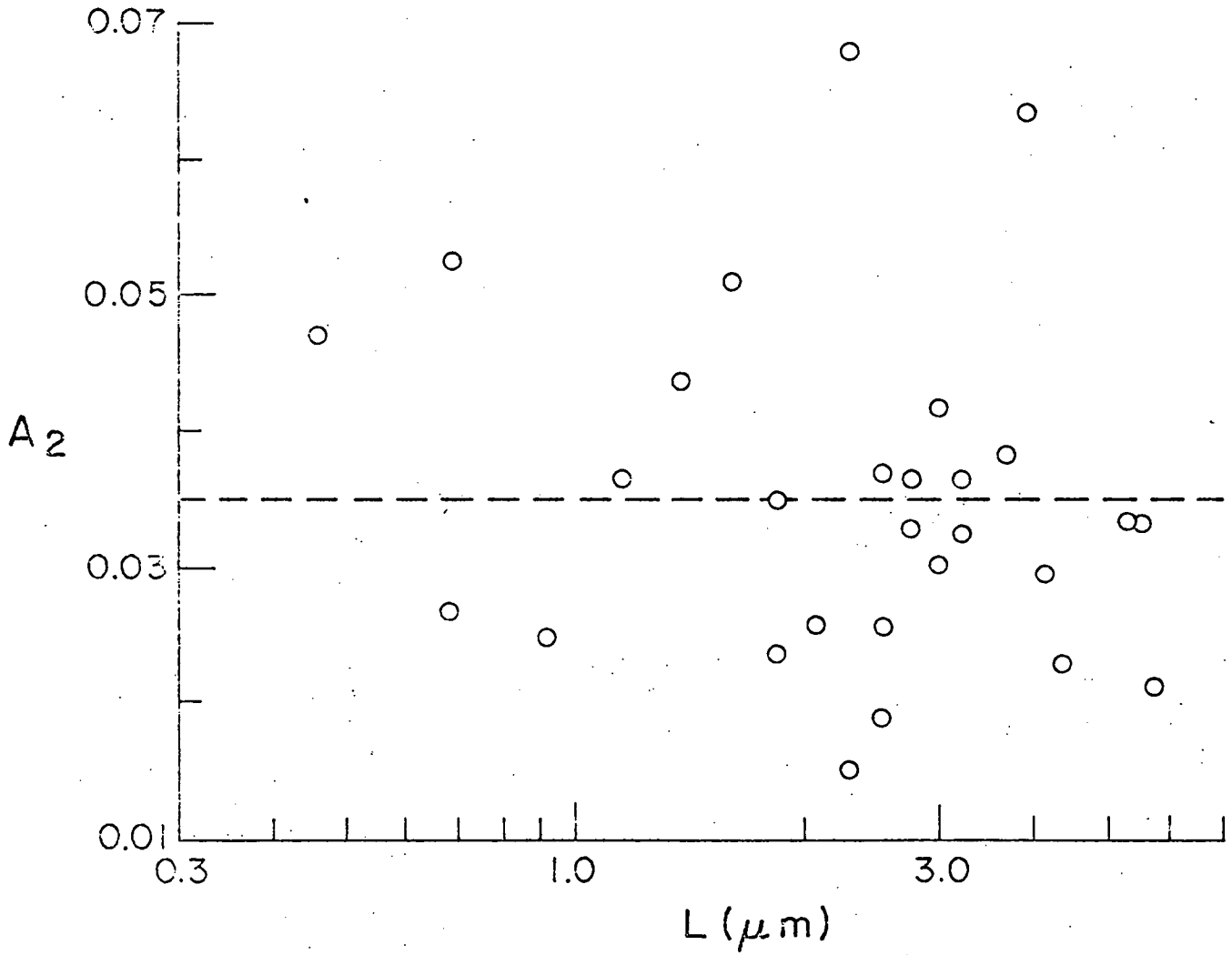

Fig. 8. Coexistence curve coefficient A_2 versus film thickness.

a film thickness dependence of A_2 is not obvious from the plot we believe that A_2 is a function of L and that this dependence is largely masked by the scatter. Figure 9 is a plot of the $A_2' = A_2[T_{c2}(L)]^{-\beta_2}$ values found by fitting the data sets. This plot is more suggestive of an L dependence. The dashed line in Fig. 9 is the average value of A_2'. This possible dependence of A_2 or A_2' upon L will be discussed further in this section.

5.2 $[T_{c3}(L) - T_{c2}(L)]$ results

We also obtained values for $T_{c3}(L)$ and $T_{c2}(L)$ from our analysis, and in Fig. 10 their difference, $T_{c3}(L) - T_{c2}(L)$, is plotted as a function of film thickness. There is a significant difference between the two critical temperatures at the smaller film thicknesses. As the film thickness increases the difference between the two critical temperatures goes to zero. The line drawn through the data in Fig. 10 is the result of a weighted fit of $[T_{c3}(L) - T_{c2}(L)] = CL^{-1/x}$ to the data. This fit gave values of $C = 0.0129 \pm 0.0012$ ($\mu m^{1/\nu 3}$ K) and $x = 0.64 \pm 0.09$. This value of x is close to the three dimensional value of $\nu_3 \approx 2/3$ (Stanley, 1971). This suggests that the crossover to two dimensional behavior causes a shift in critical temperature given by $[T_{c3}(L) - T_{c2}(L)] = CL^{-1/\nu 3}$. For two sets of data $-(0.5\ mK) < [T_{c3}(L) - T_{c2}(L)] < 0$. The uncertainties in these two determinations are larger than the differences. These two values were used in the fit, but do not appear in Fig. 10 since it is a logarithmic plot. Table III lists the $T_{c3}(L)$ and $T_{c2}(L)$ values found by fitting the data. It should

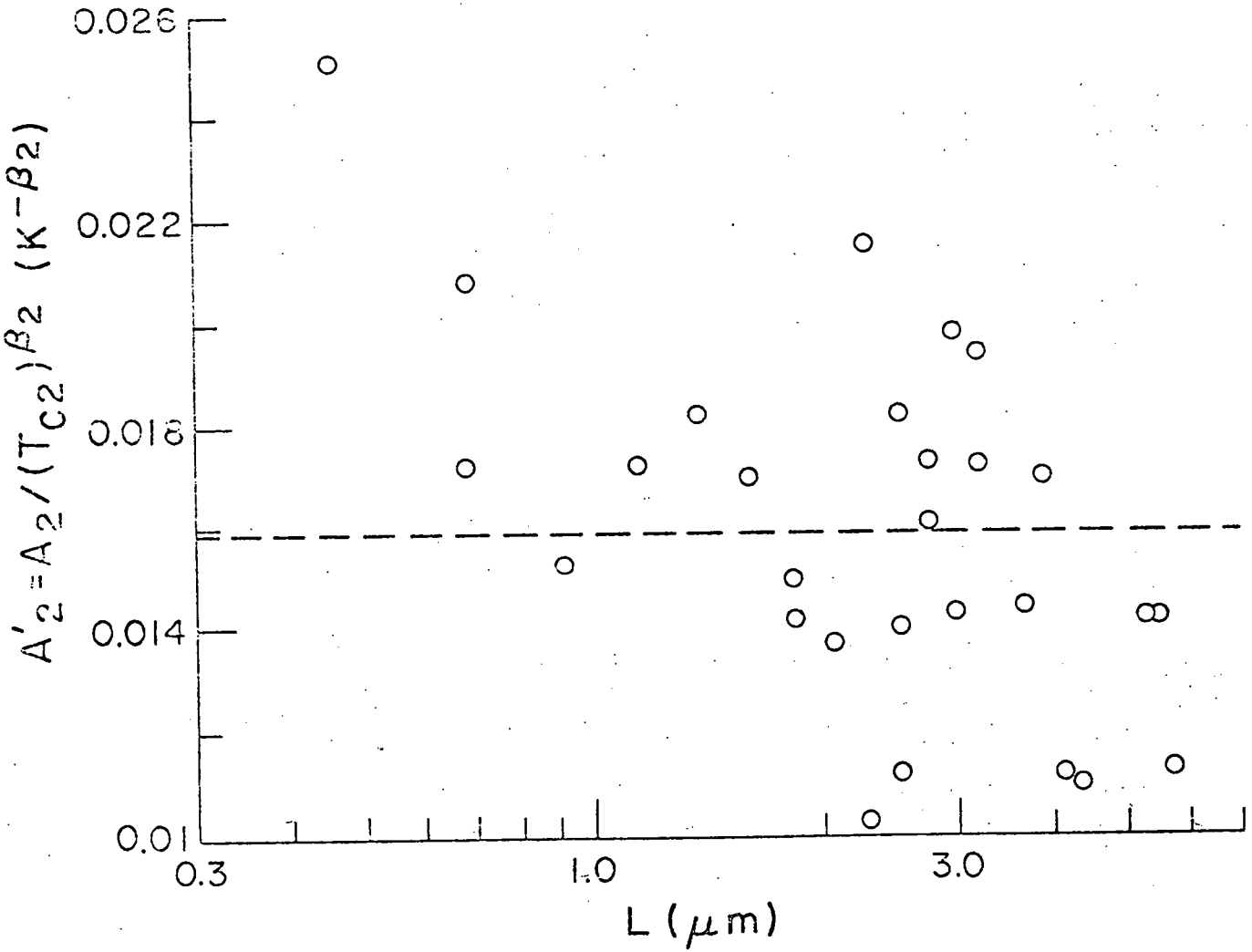

Fig. 9. Reduced coexistence curve coefficient A_2' versus film thickness.

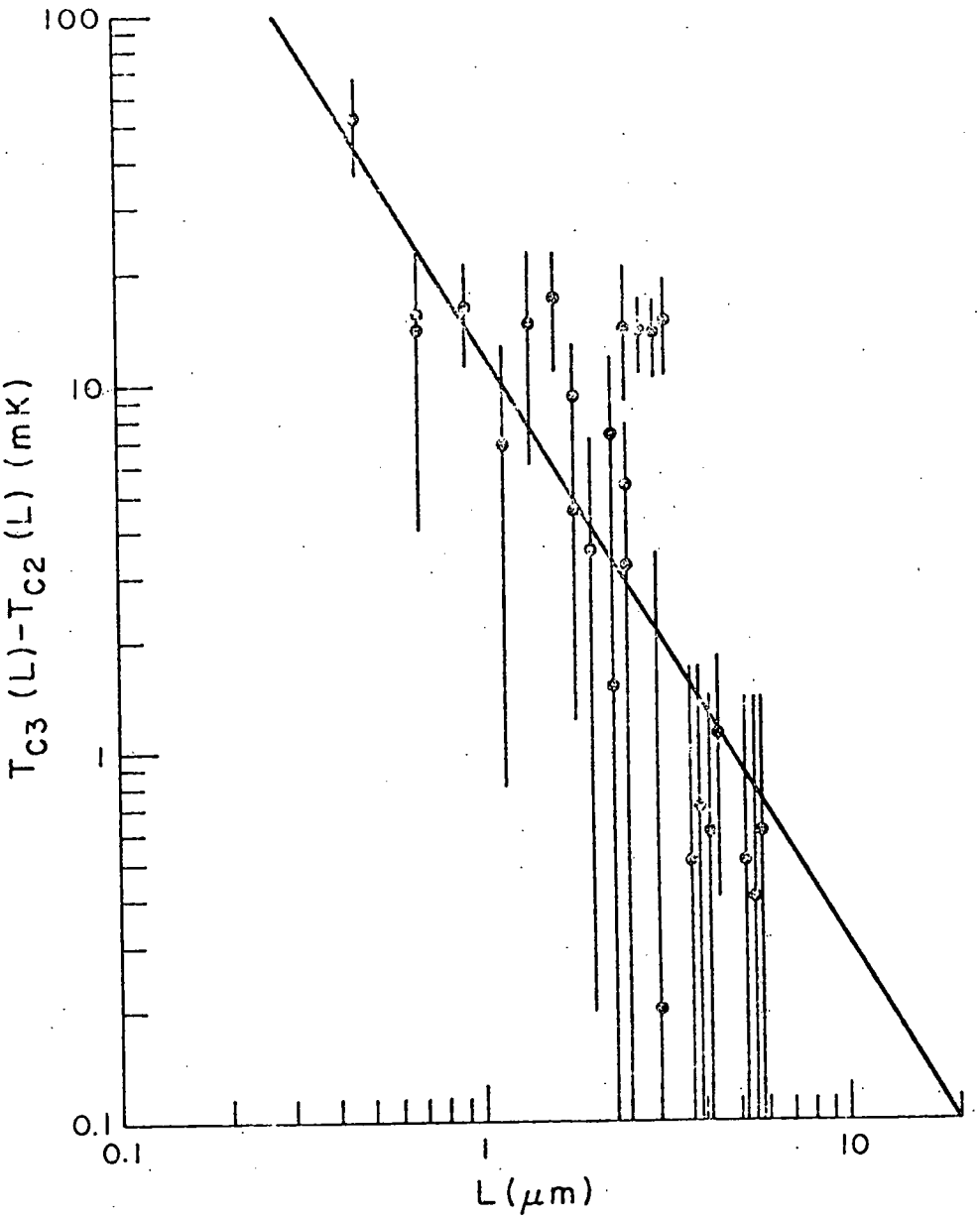

Fig. 10. $[T_{c3}(L)-T_{c2}(L)]$ versus film thickness.

TABLE III

Values for T_{c3} and T_{c2} found by fitting data taken with silver coated surfaces

Data Run	Film Thickness (μm)	T_{c3}(C)	T_{c2}(C)
1	2.28	33.9981 ± 0.004	33.9909 ± 0.0003
1	2.51	34.0022 ± 0.006	33.9881 ± 0.0003
1	2.74	34.0017 ± 0.003	33.9879 ± 0.0003
1	2.97	34.0018 ± 0.003	33.9881 ± 0.0003
1	3.20	34.0033 ± 0.004	33.9885 ± 0.0003
2	2.51	34.0244 ± 0.003	34.0212 ± 0.0003
2	2.74	34.0209 ± 0.003	34.0212 ± 0.0003
2	2.97	34.0211 ± 0.003	34.0209 ± 0.0003
2	3.20	34.0199 ± 0.004	34.0203 ± 0.0003
3	1.83	34.0126 ± 0.003	34.0081 ± 0.0003
3	2.06	34.0159 ± 0.003	34.0124 ± 0.0003
3	2.28	34.0109 ± 0.002	34.0094 ± 0.0003
3	2.51	34.0136 ± 0.003	34.0083 ± 0.0003
3	2.74	34.0102 ± 0.004	insufficient data
4	0.69	34.0379 ± 0.007	34.0226 ± 0.001
4	0.91	34.0333 ± 0.004	34.0173 ± 0.001
4	1.14	34.0196 ± 0.005	34.0128 ± 0.001
5	5.25	33.9965 ± 0.0006	33.9960 ± 0.0003
5	5.48	33.9964 ± 0.0007	33.9960 ± 0.0003
5	5.71	33.9966 ± 0.0005	33.9960 ± 0.0003
6	14.39	33.9892 ± 0.0003	no 2d region
6	14.62	33.9891 ± 0.0003	no 2d region
6	14.85	33.9892 ± 0.0003	no 2d region
7	1.37	34.0158 ± 0.008	34.0013 ± 0.0003
7	1.60	34.0183 ± 0.005	34.0011 ± 0.0003
7	1.83	34.0103 ± 0.003	34.0011 ± 0.0003
8	3.66	33.9983 ± 0.0007	33.9978 ± 0.0005
8	3.88	33.9985 ± 0.0005	33.9978 ± 0.0005
8	4.11	33.9984 0.0003	33.9978 ± 0.0005
8	4.34	33.9983 0.0004	33.9972 ± 0.0003
9	0.46	34.1063 0.010	34.0544 ± 0.005
9	0.69	34.0331 0.005	34.0191 ± 0.005

be noted that the $T_{c2}(L)$ are the temperatures where phase separation actually occurs. The $T_{c3}(L)$ temperatures lie within the 2d regions and are determined only by fitting to data outside the 2d region.

5.3 Crossover points

By plotting the data as in Fig. 4 with the accompanying 2d coexistence curve fits we can examine the crossover regions more closely. It is not clear how the 2d and 3d regions join at the crossovers because of the scatter in the data. In order to assign a unique crossover temperature to each data set we have assumed that a sharp continuous crossover occurs at the temperature where the 2d and 3d coexistence curves intersect. The crossover temperatures defined in this way lie within the previous subjectively defined crossover regions. We assume at the crossovers that $\Delta n_2 = \Delta n_3$, or

$$A_2(L)\left(\frac{T_x(L) - T_{c2}(L)}{T_{c2}(L)}\right)^{\beta_2} = A_3(L)\left(\frac{T_x(L) - T_{c3}(L)}{T_{c3}(L)}\right)^{\beta_3}, \qquad (5.1)$$

Where $T_x(L)$ is the crossover temperature. Using this expression and the results of the previous fits we have found T_x for each of the data sets. These $T_x(L)$ values are listed in Table IV.

Figure 11 is a plot of the $[T_x(L) - T_{c3}(L)]$ values found by the above process. The error bars on $T_x(L)$ span the subjective crossover regions defined earlier. One of our original expectations was that crossovers might occur when the correlation length of the film was approximately equal to the film thickness; that is, when

TABLE IV

Values for T_x found for data taken with silver coated surfaces

Data Run	Film Thickness (μm)	T_x(C)
1	2.28	34.0076 ± 0.005
1	2.51	34.0067 ± 0.003
1	2.74	34.0103 ± 0.005
1	2.97	34.0089 ± 0.005
1	3.20	34.0106 ± 0.005
2	2.51	34.0342 ± 0.005
2	2.74	34.0314 ± 0.005
2	2.97	34.0346 ± 0.004
2	3.20	34.0349 ± 0.006
3	1.83	34.0219 ± 0.004
3	2.06	34.0226 ± 0.004
3	2.28	34.0171 ± 0.003
3	2.51	34.0212 ± 0.004
4	0.69	34.0575 ± 0.010
4	0.91	34.0547 ± 0.007
4	1.14	34.0314 ± 0.005
5	5.25	33.9990 ± 0.001
5	5.48	33.9990 ± 0.001
5	5.71	33.9990 ± 0.001
7	1.37	34.0242 ± 0.003
7	1.60	34.0248 ± 0.003
7	1.83	34.0147 ± 0.003
8	3.66	33.9993 ± 0.0005
8	3.88	33.9993 ± 0.0005
8	4.11	33.9991 ± 0.0005
8	4.34	33.9997 ± 0.0004
9	0.46	34.1379 ± 0.010
9	0.69	34.0607 ± 0.008

$L = m\xi_3$, where $m \simeq 1$. This relation predicts that

$$[T_x(L) - T_{c3}(L)] = [T_{c3}(L)(m\xi_{03})^{1/\nu_3}]L^{-1/\nu_3} \quad . \qquad (5.2)$$

Accordingly, we have fit $T_x(L) - T_{c3}(L) = D_3 L^{-1/y_3}$ to the data in Fig. 11 and find $D_3 = 0.0127 \pm 0.0010$ ($\mu m^{1/\nu_3}$ K), $y_3 = 0.66 \pm 0.06$. This fit is the solid line in Fig. 11. The y_3 value is very close to $\nu_3 \approx 2/3$. The values for D_3 and y_3 give $m\xi_o = 13$ Å $\pm$ 8 Å. Using Gülari's (1972) value of $\xi_o = 2.9$ Å for 2,6-lutidine + water, this result implies that m lies between 2 and 7. Thus we are observing crossovers at temperatures where the correlation length of the film is a significant fraction of the film thickness.

We have also fit $[T_x(L) - T_{c2}(L)] = D_2 L^{-1/y_2}$ to the data and find $D_2 = 0.0264 \pm 0.0016$ ($\mu m^{1/\nu_3}$ K) and $y_2 = 0.61 \pm 0.06$. As before the value for y_2 is close to ν_3. The $[T_x(L) - T_{c2}(L)]$ versus L data are plotted in Fig. 12. The solid line in Fig. 12 is the result of the above fit. It is perhaps not surprising that $[T_x(L) - T_{c2}(L)]$ has this functional dependence, since $T_x - T_{c2} = (T_x - T_{c3}) + (T_{c3} - T_{c2})$, and as we have seen earlier, apparently $[T_{c3} - T_{c2}] = CL^{-1/\nu_3}$.

To obtain values for $T_x(L)$ we have used the assumption that $\Delta n_2 = \Delta n_3$ at the crossovers. This implies that the ratio A_2/A_3 is a function of the film thickness, L_3 which can be seen from the condition

$$A_2 \left(\frac{T_x - T_{c2}}{T_{c2}} \right)^{\beta_2} = A_3 \left(\frac{T_x - T_{c3}}{T_{c3}} \right)^{\beta_3} \quad , \qquad (5.3)$$

written as

$L = m\xi_3$, where $m \simeq 1$. This relation predicts that

$$[T_x(L) - T_{c3}(L)] = [T_{c3}(L)(m\xi_{03})^{1/\nu_3}]L^{-1/\nu_3} \quad . \tag{5.2}$$

Accordingly, we have fit $T_x(L) - T_{c3}(L) = D_3 L^{-1/y_3}$ to the data in Fig. 11 and find $D_3 = 0.0127 \pm 0.0010$ ($\mu m^{1/\nu_3}$ K), $y_3 = 0.66 \pm 0.06$. This fit is the solid line in Fig. 11. The y_3 value is very close to $\nu_3 \approx 2/3$. The values for D_3 and y_3 give $m\xi_o = 13$ Å $\pm$ 8 Å. Using Gülari's (1972) value of $\xi_o = 2.9$ Å for 2,6-lutidine + water, this result implies that m lies between 2 and 7. Thus we are observing crossovers at temperatures where the correlation length of the film is a significant fraction of the film thickness.

We have also fit $[T_x(L) - T_{c2}(L)] = D_2 L^{-1/y_2}$ to the data and find $D_2 = 0.0264 \pm 0.0016$ ($\mu m^{1/\nu_3}$ K) and $y_2 = 0.61 \pm 0.06$. As before the value for y_2 is close to ν_3. The $[T_x(L) - T_{c2}(L)]$ versus L data are plotted in Fig. 12. The solid line in Fig. 12 is the result of the above fit. It is perhaps not surprising that $[T_x(L) - T_{c2}(L)]$ has this functional dependence, since $T_x - T_{c2} = (T_x - T_{c3}) + (T_{c3} - T_{c2})$, and as we have seen earlier, apparently $[T_{c3} - T_{c2}] = CL^{-1/\nu_3}$.

To obtain values for $T_x(L)$ we have used the assumption that $\Delta n_2 = \Delta n_3$ at the crossovers. This implies that the ratio A_2/A_3 is a function of the film thickness, L_3 which can be seen from the condition

$$A_2 \left(\frac{T_x - T_{c2}}{T_{c2}} \right)^{\beta_2} = A_3 \left(\frac{T_x - T_{c3}}{T_{c3}} \right)^{\beta_3} \quad , \tag{5.3}$$

written as

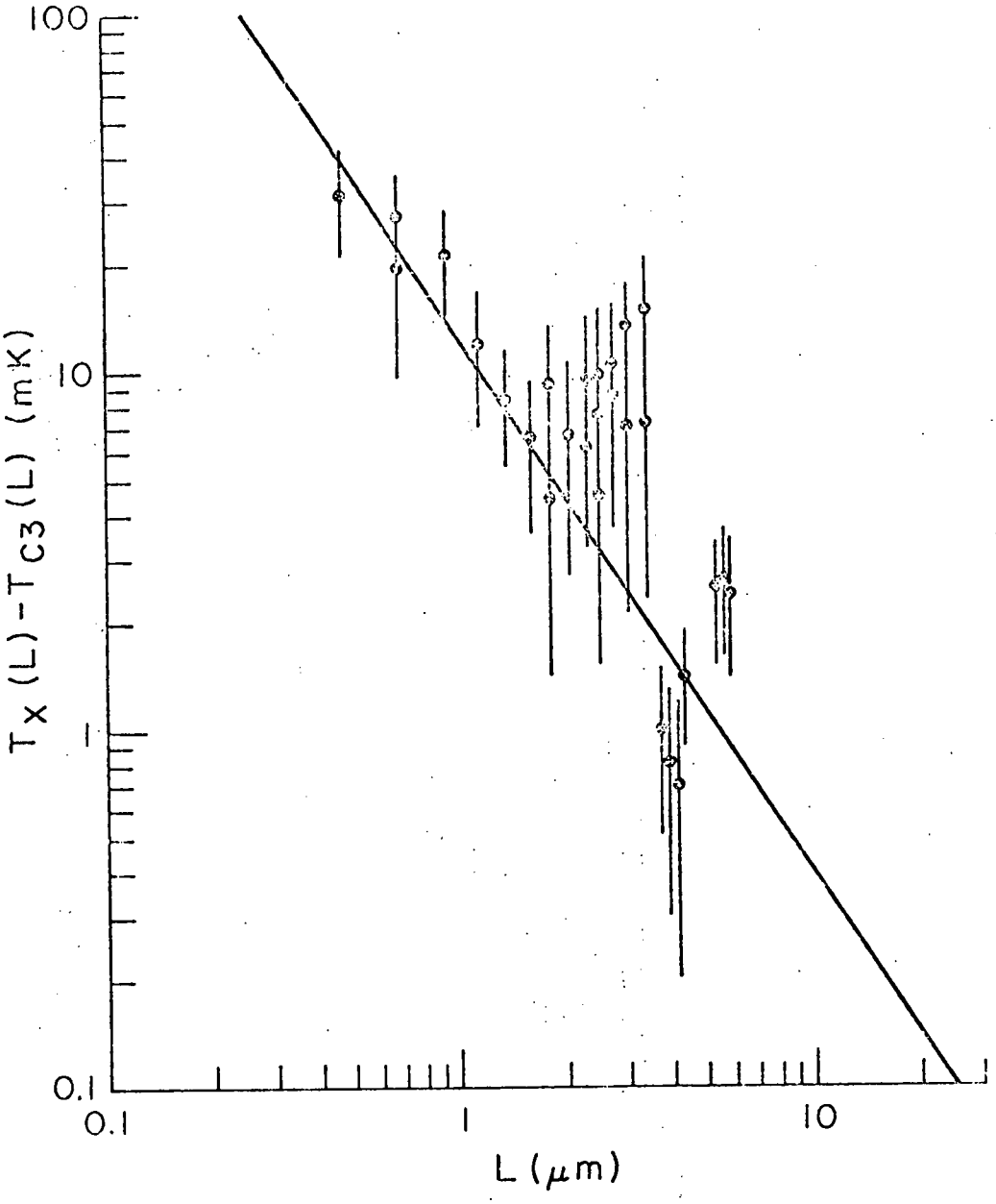

Fig. 11. $[T_x(L)-T_{c3}(L)]$ versus film thickness.

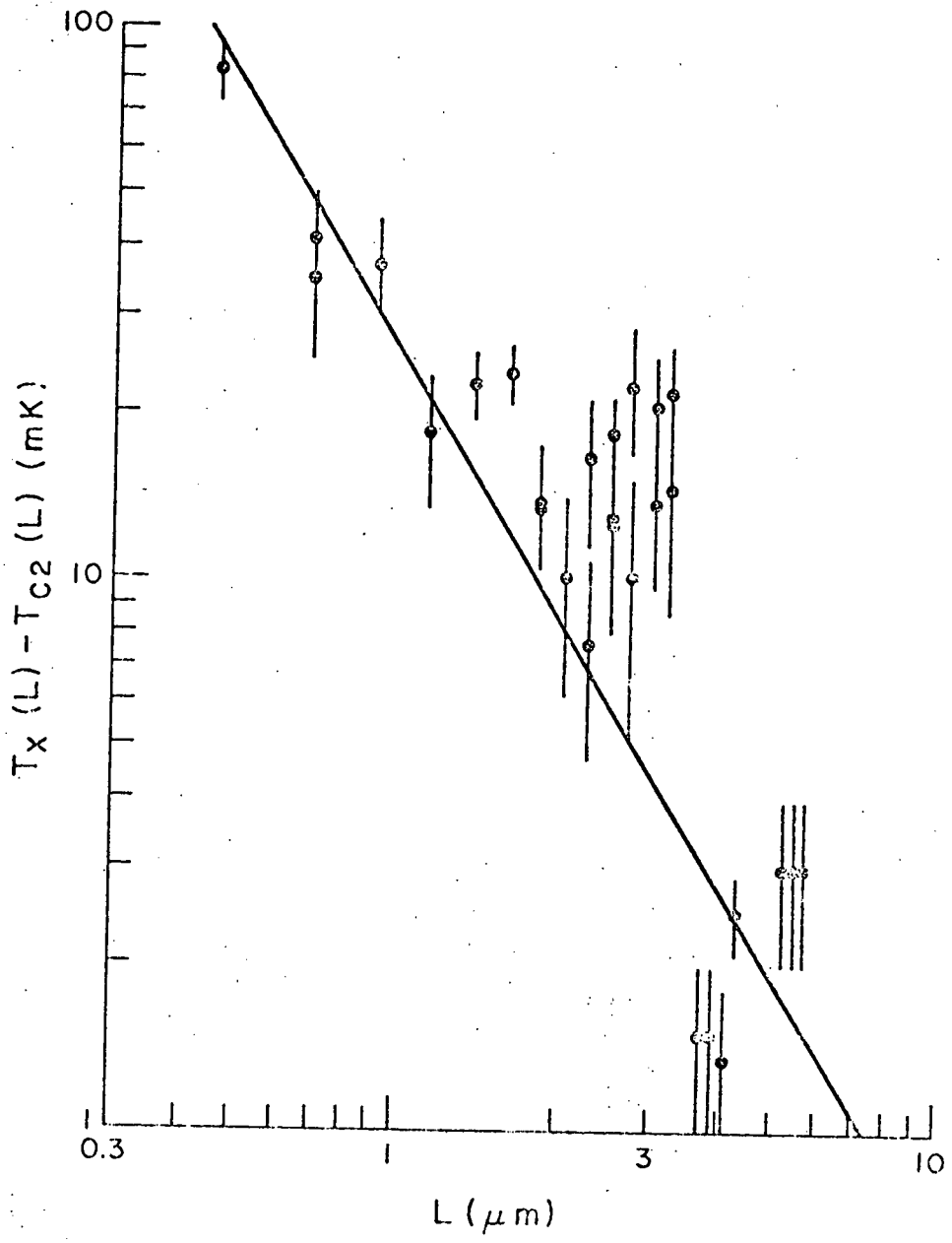

Fig. 12. $[T_x(L)-T_{c2}(L)]$ versus film thickness.

$$A_2/A_3 = \frac{T_{c2}^{\beta_2}}{T_{c3}^{\beta_3}} \frac{(T_x - T_{c3})^{\beta_3}}{(T_x - T_{c2})^{\beta_2}} \quad . \tag{5.4}$$

We have found above that $T_x - T_{c3} = D_3 L^{-1/\nu_3}$ while $T_x - T_{c2} = D_2 L^{-1/\nu_3}$. In addition, $T_{c2}^{\beta_2}/T_{c3}^{\beta_3} \approx [T_c(\infty)]^{\beta_2-\beta_3}$, which is independent of L. Combining these results we find that the L dependence of A_2/A_3 is given by

$$A_2/A_3 = EL^{(\beta_2-\beta_3)/\nu_3} \quad , \tag{5.5}$$

where $E = (T_{c2}/D_2)^{\beta_2}(D_3/T_{c3})^{\beta_3}$. Fisher (1971) has predicted a thickness dependence in the coefficient of the susceptibility of a ferromagnetic film. If his scaling arguments are applied to the coefficients of the coexistence curves they suggest that $A_2/A_3 \propto L^{(\beta_2-\beta_3)/\nu_3}$, which is the result we found above. Figure 13 is a plot of the actual A_2/A_3 ratios found for the various data sets. The solid line represents the ratios predicted by the above expression, using the average values of β_2 and β_3, the values for D_2 and D_3 found above, $\nu_3 = 0.64$ and $T_{c2} = T_{c3} = 307$ K. Although there is obviously too much scatter in the data to verify the above prediction, the solid line does seem to fit the general trend apparent in the data.

One final point to be made concerning the crossover behavior involves a hysteresis that was observed. In some cases the Δn measurements were made by monotonically increasing the temperature. In other cases the temperature was randomly raised and lowered to

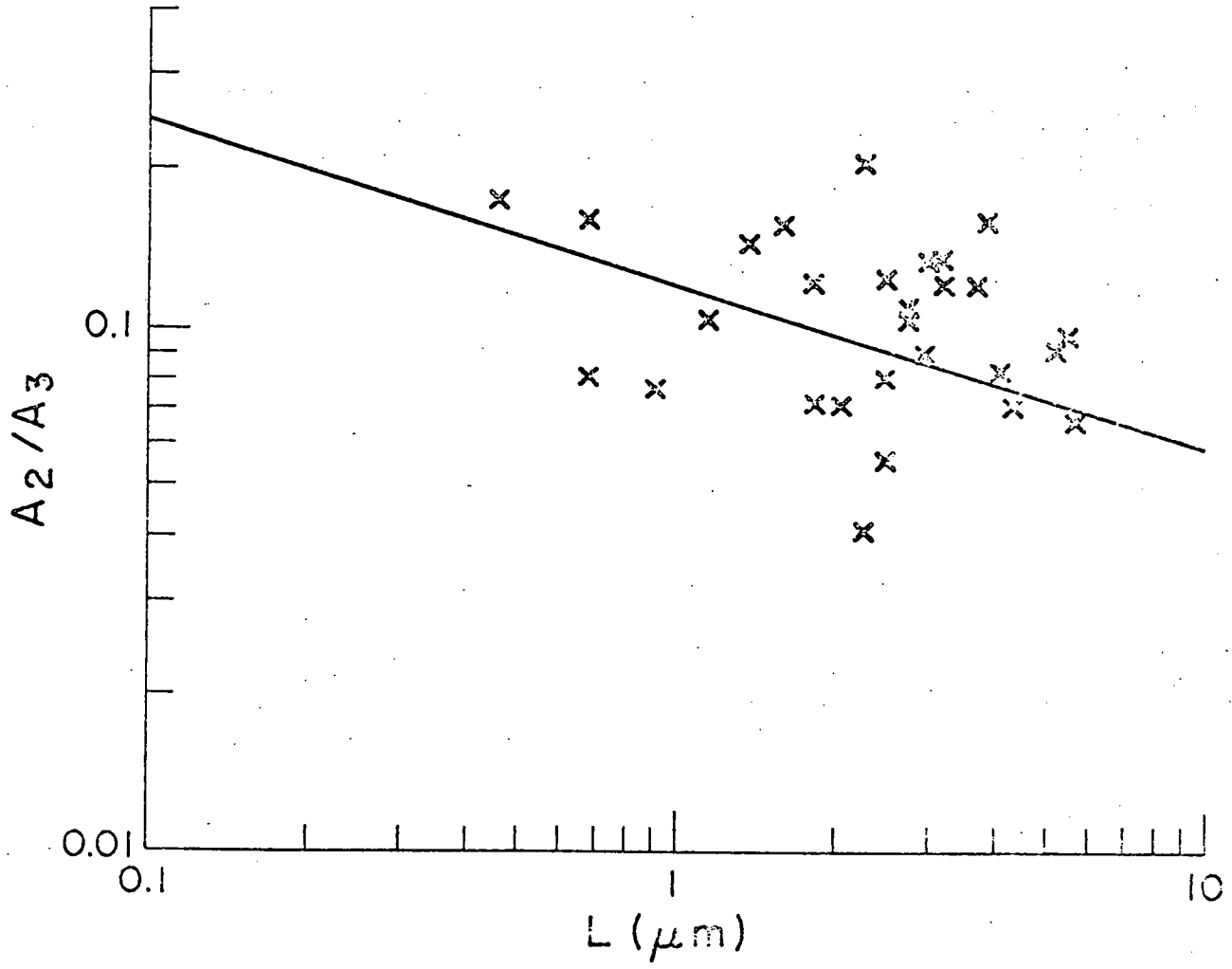

Fig. 13. A_2/A_3 versus film thickness.

make the measurements. We found that as long as the temperature remained in the 2d region the Δn measurements were reproducible. If the temperature was raised into the 3d region, however, and then lowered back into the 2d region, in some cases the fluids continued to behave as 3d fluids even below the crossover. For all film thickness less than 6 μm we have observed crossovers from 2d to 3d behavior as the temperature is raised (moving away from the critical point). However, for some films the crossover from 3d to 2d is not observed when the temperature is lowered toward the critical point.

5.4 Critical temperature shifts

The experiments show that for the silver surfaces critical temperatures increase as L decreases. Figure 14 is a plot of this shift in critical temperature, $[T_{c3}(L) - T_{c3}(\infty)]$, as a function of L, where $T_{c3}(\infty)$ is the bulk value of the critical temperature and was determined by a process to be described below. The critical temperatures, $T_{c3}(L)$, used in Fig. 14 were determined in three ways [the $T_{c3}(L)$ values are listed in Tables III and V]. For L larger than 10 μm, $T_{c3}(L)$ was determined by observing the fringes disappear. For values of L between 6 and 10 μm $T_{c3}(L)$ was determined by observation of the fringe splitting. For thicknesses of less than 6 μm $T_{c3}(L)$ was found by fitting the 3d data. At spacings of 14.4, 14.6, and 14.9 μm the fringes disappeared at the critical point and reappeared as split fringes. Δn was measured as a function of temperature for these fringes and showed no

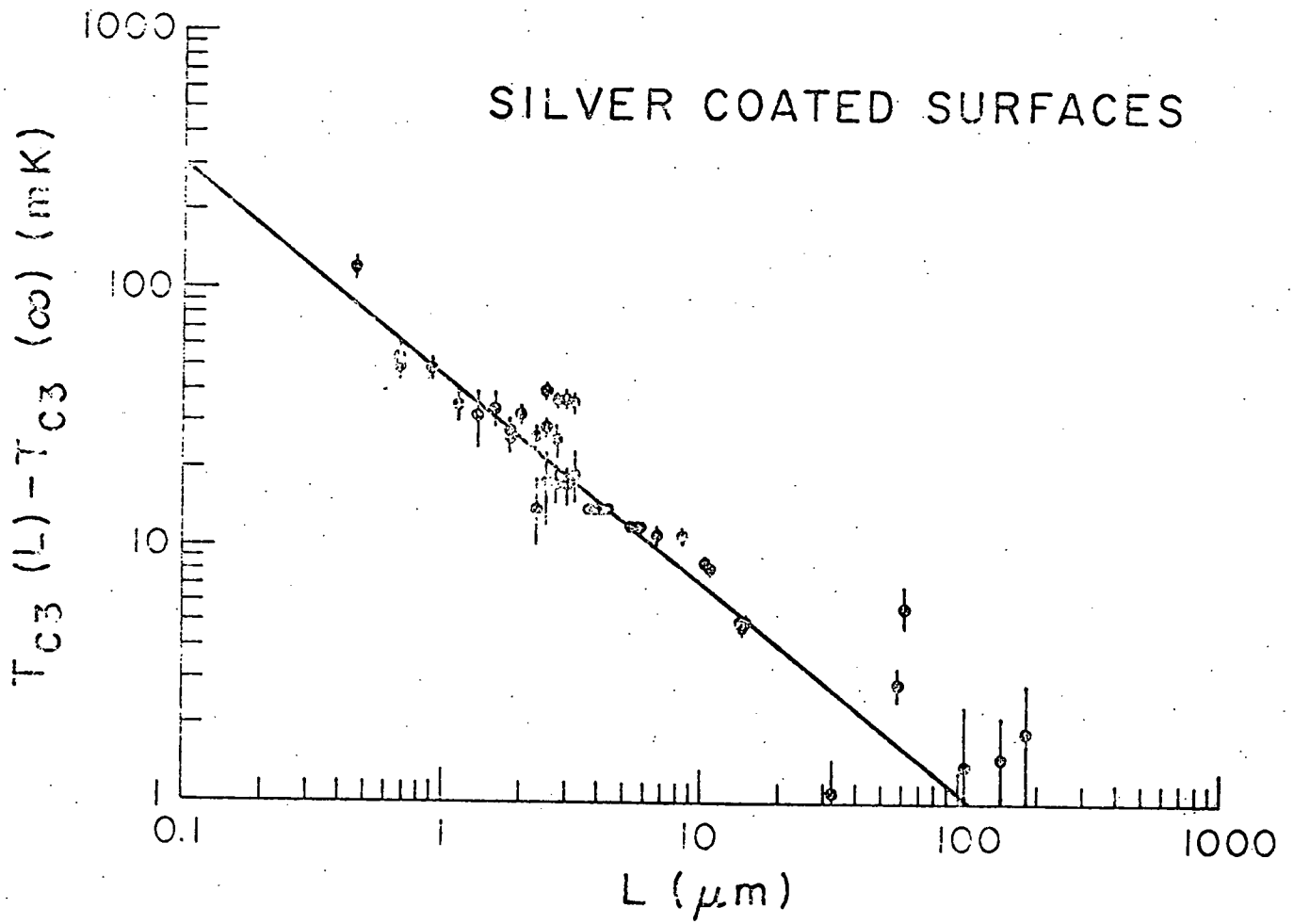

Fig. 14. $[T_{c3}(L)-T_{c3}(\infty)]$ versus film thickness for silver surfaces.

TABLE V

Values for T_{c3} found by means other than fitting for data taken with silver surfaces

Film Thickness (μm)	T_{c3}(C)
32	33.9853 ± 0.0004
61	33.9900 ± 0.001
8.4	33.9953 ± 0.0005
182	33.9861 ± 0.001
144	33.9857 ± 0.0007
106	33.9856 ± 0.001
59	33.9871 ± 0.0005
10.3	33.9927 ± 0.0004
10.6	33.9923 ± 0.0006
130	33.9850 ± 0.003
6.7	33.9955 ± 0.001
14.39	33.9895 ± 0.0003
14.62	33.9891 ± 0.0003
14.85	33.9892 ± 0.0003

2d behavior, only 3d behavior. The $T_{c3}(L)$ values found by fitting these data fell within the error bars on the $T_{c3}(L)$ values found from the disappearance of the fringes. This gives us a basis for assuming that the $T_{c3}(L)$ values found by observing the fringe disappearance are the same as $T_{c3}(L)$ values that would be found by fitting Δn versus temperature data.

In the range $6\ \mu m \leq L \leq 10\ \mu m$ the refractive index resolution is such that the onset of fringe splitting can be specified to ± 0.1 mK. Results presented above indicate that at these thicknesses $T_{c3}(L) - T_{c2}(L) < 0.7$ mK, and so we have assumed that for this film thickness range the temperature at which the fringes split is approximately $T_{c3}(L)$.

The solid line in Fig. 14 is the result of fitting $T_{c3}(L) = T_{c3}(\infty) + FL^{-\lambda}$ to the $T_{c3}(L)$ versus L data [$T_{c3}(\infty)$ is a parameter determined by the fit]. This fit gave values of $\lambda = 0.81 \pm 0.08$, $F = 0.047 \pm 0.002$ (μm^{λ} K), and $T_{c3}(\infty) = 33.9842 \pm 0.0008$ C. The value $\lambda = 0.81$ suggests a stronger finite size - bounding surface effect upon T_c than is suggested by the work of Domb (1973) and Binder (1972) for a layered Ising lattice, where $\lambda \approx 1$. The data in Fig. 14 show considerable scatter and the reduced χ^2 per point for the fit is approximately 6. This indicates that our preparation technique still is not producing fluid films of exactly the same composition.

5.5 Results with dielectric coatings

The interpretation of the data taken with the dielectric coated flats is complicated by several experimental factors. First, these data were taken while developing our sample preparation techniques and so much of the data were taken with poorly prepared samples. Second, the SiO_2 protective overcoat on each flat was presumed to be one wavelength thick. In retrospect, however, several observations made at the time suggest that the overcoat was perhaps two wavelengths thick on each flat. Since the fluids destroyed the coatings on the flats we could not measure the thickness of the SiO_2 layer to resolve this uncertainty. This leads to an uncertainty of 0.9 μm in the film thickness. Finally, far fewer split fringe measurements were made with these coatings than with the silver coated flats. While measurements of Δn were made for six film thicknesses, the average data set contained only 11 points. This made it impossible to apply the analysis scheme that we used with the silver coated flat data.

Despite the above difficulties we have been able to determine the behavior of the critical temperature as a function of film thickness. In this analysis we have only used data taken at film thicknesses larger than 8 μm. Thus the uncertainty in the film thickness is relatively unimportant. As for the poor preparation, we have observed that although this causes increased scatter in the T_c measurements the effect is most dramatic at very small L. At larger L this scatter seems to have no systematic effect on the

results. The $T_{c3}(L)$ values observed with dielectric surfaces are listed in Table VI.

As with the silver data, we have fit the dielectric critical temperatures with $T_{c3}(L) = T_{c3}(\infty) + FL^{-\lambda}$. We find $T_{c3}(\infty) = 33.9750 \pm 0.0012$ C, $F = -0.24 \pm 0.05$ (μm^{λ} C) and $\lambda = 0.80 \pm 0.09$. Figure 15 is a plot of the shift in critical temperature, $T_{c3}(L) - T_{c3}(\infty)$, as a function of film thickness for the dielectric flats. The solid line is the result of the fit to the data. The above form provides an adequate description of the data. The values for $T_{c3}(\infty)$ for the silver and dielectric data sets differ by 9 mK. As described earlier, experimental problems limit comparison of absolute temperatures between the two data sets to ±10 mK. Thus the difference in $T_{c3}(\infty)$ values is reasonable. The values of λ for silver and dielectric coatings are 0.81 and 0.80 respectively. This suggests that λ does not depend upon the specific surfaces. The coefficient F differs markedly for the two coatings. The two values differ in magnitude by a factor of 5 and also differ in sign. This has the remarkable effect that for the silver surfaces the critical temperature rises, while for the SiO_2 overcoated dielectric surfaces the critical temperature falls as the film thickness is reduced. Obviously, the coefficient F depends strongly upon the specific nature of the surfaces in contact with the fluids. In a separate simple experiment we have observed that in the two phase region the lutidine rich phase preferentially wets silver surfaces while the water rich phase preferentially wets quartz surfaces. This indicates that for our fluids the surface

TABLE VI

Values for T_{c3} found for data taken with dielectric surfaces

Film Thickness (μm)	T_{c3}(C)
110	33.9682 ± 0.0003
72	33.9653 ± 0.0005
12.6	33.9380 ± 0.0007
8.0	33.9280 ± 0.001
272	33.9717 ± 0.0015
272	33.9728 ± 0.0003
138	33.9698 ± 0.0004
69	33.9690 ± 0.001
48	33.9608 ± 0.0004
33	33.9581 ± 0.0007
242	33.9715 ± 0.0004
174	33.9719 ± 0.0003
214	33.9721 ± 0.001
199	33.9680 ± 0.002
199	33.9726 ± 0.001
199	33.9708 ± 0.001
199	33.9719 ± 0.002
215	33.9713 ± 0.001
216	33.9730 ± 0.001
139	33.9698 ± 0.001
95	33.9686 ± 0.004
58	33.9661 ± 0.0004
36	33.9622 ± 0.0004
18	33.9526 ± 0.0003
117	33.9696 ± 0.001
78	33.9682 ± 0.001
45	33.9641 ± 0.001
170	33.9720 ± 0.0005
250	33.9725 ± 0.0004
236	33.9729 ± 0.0006
26	33.9573 ± 0.001
18	33.9540 ± 0.0005

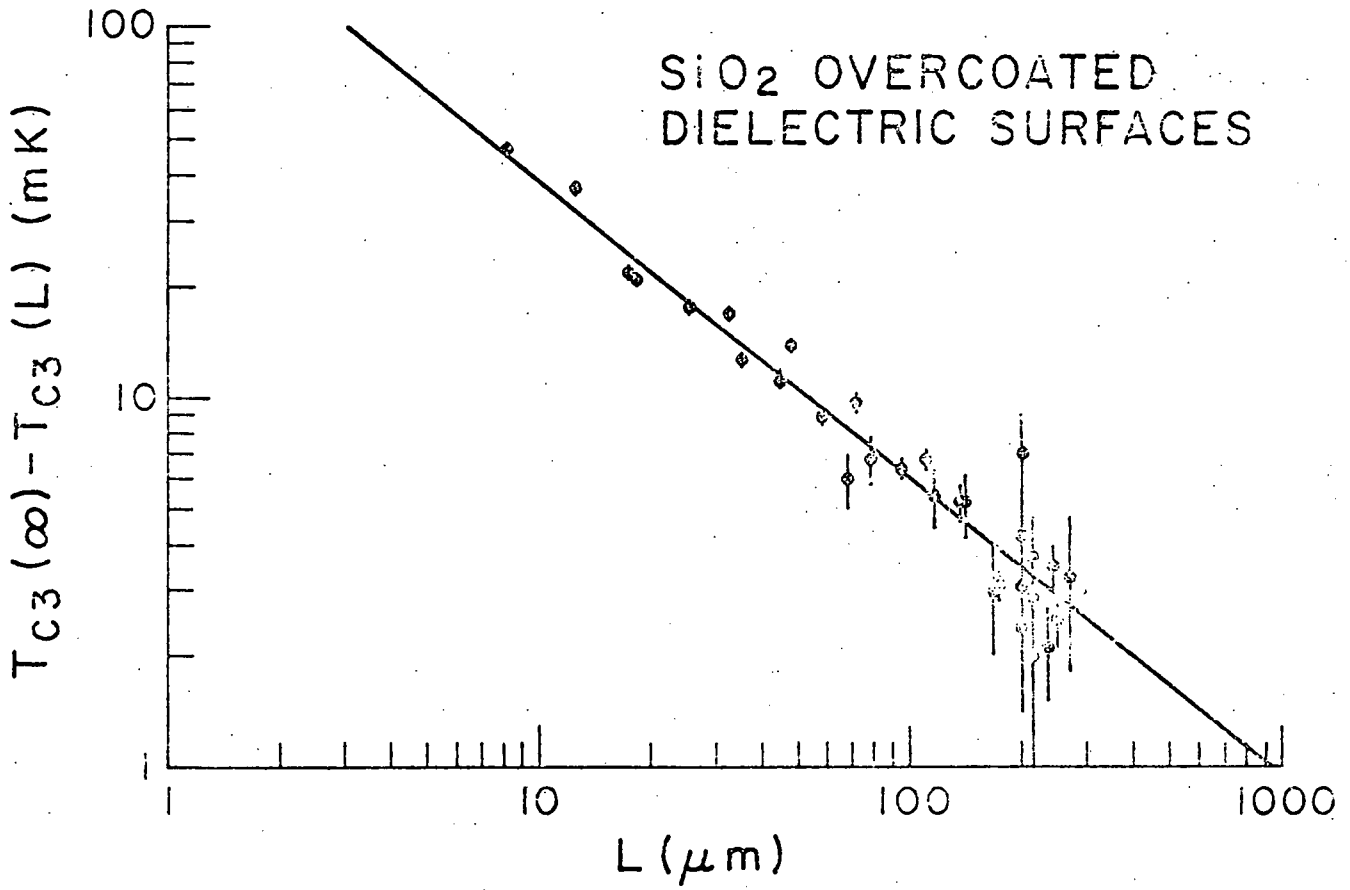

Fig. 15. $[T_{c3}(\infty)-T_{c3}(L)]$ versus film thickness for dielectric coated surfaces.

effects change significantly when silver surfaces are substituted for SiO_2 overcoated dielectric surfaces. This change may cause the observed change in amplitude of the $T_{c3}(L)$ dependence.

With the dielectric coated flats, split fringe measurements were made at five film thicknesses of less than 5 μm. Since the film thickness must be known to convert the fringe position measurements into Δn values, the uncertainty in the spacing mentioned above makes the absolute magnitude of these Δn values very uncertain. If the data were fit, this would result in a large uncertainty in the coefficient A of the coexistence curve. Since there is so little data in each of these data sets, however, we have not been able to fit the data as we did the silver data. When we plot these data as is Fig. 4, though, several qualitative observations can be made. All five of these data sets show crossovers. From the plots, T_{c2}, T_{c3}, and T_x can be estimated. $T_{c3} - T_{c2} \geq 0$ for each of these sets. $T_x - T_{c2}$ is a monotonic function of temperature and increases as L decreases. The exact functional dependence of these quantities upon film thickness cannot be determined because of the uncertainty in film thickness. These results for the SiO_2 overcoated dielectric flats agree with the conclusions reached with the silver coated flats.

CHAPTER VI

SUMMARY AND OUTLOOK

6.1 A summary of our results

We have performed refractive index studies on films of a critical mixture of 2,6-lutidine+water confined between reflecting optical flats, in the film thickness range ~0.4 μm to ~300 μm. Above the critical temperature of these films, in the two phase region, we have measured Δn, the difference between the indexes of refraction of the two phases. Since to a close approximation Δn is proportional to the order parameter, measurements of Δn as a function of temperature map out the coexistence curves of the films. For each film of thickness less than 6 μm, we observe an apparent crossover near the critical point from three dimensional to two dimensional scaling behavior. That is, for each film there is a crossover temperature, T_x, below which the coexistence curve is characterized by $\beta \approx 1/8$, and above which $\beta \approx 1/3$. We find a weighted average value for β below T_x of 0.126 ± 0.005, and a weighted average for β above T_x of 0.332 ± 0.003. The coefficient, A_2, of the 2d coexistence curve seems to depend upon the film thickness as predicted: $A_2 \propto L^{(\beta_2-\beta_3)/\nu_3}$.

The dependence of the crossover temperatures upon film thickness, L, appears to be given by $T_x(L) - T_{c3}(L) = D_3 L^{-1/\nu_3}$. $T_{c3}(L)$ is an effective critical temperature found by fitting to

the 3d part of the coexistence curve for a film of thickness L, and ν_3 is the 3d Ising model correlation length critical exponent. In our studies, the crossovers from 3d to 2d seem to occur when $\xi_{3d} \simeq (1/4)L$. We find that $T_{c2}(L)$, the critical temperature for thickness L found by fitting to the 2d part of the coexistence curve, differs from $T_{c3}(L)$. The difference appears to scale with L as $T_{c3}(L) - T_{c2}(L) = CL^{-1/\nu_3}$. $T_{c3}(L)$ is related to the film thickness by $T_{c3}(L) = T_{c3}(\infty) + FL^{-\lambda}$. Data taken with silver coated surfaces over a film thickness range of 0.46 μm to 182 μm give the values $\lambda = 0.81 \pm 0.09$, $F = 0.047 \pm 0.002$ (μm^{λ} K). Data taken with SiO_2 overcoated dielectric surfaces over a range of film thicknesses from 8 μm to 272 μm give $\lambda = 0.80 \pm 0.08$, $F = -0.24 \pm 0.05$ (μm^{λ} K). These two results for λ indicate an enhanced finite size effect over that estimated by Binder (1972) or Domb (1973). The two types of surfaces cause the critical temperatures to shift in opposite directions. The silver surfaces raise the critical temperature as the fluid film thickness is decreased, while the dielectric surfaces lower the critical temperature as the fluid film thickness decreases. The magnitudes of the shifts with the dielectric surfaces are approximately five times larger than the shifts with the silver surfaces.

In general, the results of our measurements support scaling theory predictions of thick film critical behavior to a surprising degree. By fitting the $T_x(L) - T_{c3}(L)$ data, the $T_{c3}(L) - T_{c2}(L)$ data and the $T_x(L) - T_{c2}(L)$ data we obtained the following specific results:

$$T_x(L) - T_{c3}(L) = 0.0127\ L^{-1.52} \quad , \tag{6.1}$$

$$T_{c3}(L) - T_{c2}(L) = 0.0129\ L^{-1.57} \quad , \tag{6.2}$$

and

$$T_x(L) - T_{c2}(L) = 0.0264\ L^{-1.63} \quad . \tag{6.3}$$

Since $[T_x(L) - T_{c2}(L)] = [T_x(L) - T_{c3}(L)] + [T_{c3}(L) - T_{c2}(L)]$ the above results are not independent; the third provides a check on the consistency of the first two. Assuming the exponent in each of the above expressions is $1/\nu_3'$ we obtain three values for ν_3': 0.66 ± 0.06, 0.64 ± 0.09, and 0.61 ± 0.06 (average value $\nu_3' = 0.64 \pm 0.04$). As we have mentioned in the introduction, since our measurements are made in the two phase region we expect the correlation length to be characterized by ν_3' rather than ν_3. However, we expect $\nu_3' \approx \nu_3$, and the value found for ν_3' seems to substantiate this. These values agree well with other experimental ($\nu_3 = 0.625 \pm 0.003$) (see Guillou and Zinn-Justin, 1977 and references therein) and theoretical results ($\nu_3 = 0.6300 \pm 0.0008$) (Guillou and Zinn-Justin, 1977). The results of the first two fits suggest that $T_x(L) - T_{c3}(L) = T_{c3}(L) - T_{c2}(L)$, and so $T_{c3}(L) = [T_x(L) + T_{c2}(L)]/2$. Thus, the temperature ranges bounded by $T_{c2}(L)$ and $T_x(L)$, over which we observe 2d scaling behavior are apparently symmetric about $T_{c3}(L)$. We are not aware of any constraint which should impose this symmetry.

Throughout our work we have been concerned that critically wetted surface films of the type proposed by Cahn (1977) might play a significant part in the behavior of our critical films. In

this case a film consisting primarily of one fluid phase would wet out on the solid-fluid interface, forming an intermediate layer between our optical flats and the thick film sample. Cahn has suggested that for the case of a bulk critical fluid sample in contact with a surface, such wetted layers can grow to macroscopic thicknesses. However, our experimental results are inconsistent with such behavior. We are unable to explain the crossovers to $\beta \approx 1/8$ behavior as a wetting process. The wetting layers would require a peculiar temperature dependence to yield a rather sharp crossover followed by an extended region where $\beta \approx 1/8$. Although this behavior cannot be explained by wetting, wetting might still be present modifying the behavior of the films in a less significant way. A wetting layer would cause the measured Δn values to be less than the actual refractive index difference between the two phases. If the thickness of the wetting layer was temperature dependent it would introduce an additional temperature dependence into the measured Δn values, over and above the normal coexistence curve dependence. We find however, that the measured Δn values map out normal coexistence curves with the expected values for β and no systematic deviations. Furthermore, unless the wetting layers had an unusual dependence upon film thickness, the measured Δn for a given $T - T_c$ would depend upon the film thickness. This is not observed. Thus, to within the limits of our measurements, we have observed no evidence of wetting layers.

6.2 Outlook for future work

Experimentally, there remains much to be done. Experiments using different critical fluid mixtures and different surfaces need to be done to check the generality of our results. The exact behavior of the fluids at the crossover temperatures is hidden by scatter in the data. More careful measurements are needed to determine whether the crossovers are sharp as we have assumed, or smooth, implying a finite temperature range where the behavior is neither two dimensional nor three dimensional. The suspected spacing dependence of the coefficient of the two dimensional coexistence curve needs to be checked by further experimentation.

Our experiment shows that crossovers to two dimensional behavior apparently occur in the two phase region of thick films of 2,6-lutidine+water. Different experiments need to be performed to determine whether similar crossovers occur in the one phase region near the critical temperature. These crossovers may be observed by investigating the refractive index anomaly in the one phase region or by doing correlation spectroscopy on scattered light from the film and extracting ν_2 and ν_3.

Our belief that we are seeing crossovers to two dimensional behavior rests largely on our measured values for $\beta \approx 1/8$ and the dependence of the observed crossovers upon film thickness. To confirm this belief different experiments capable of measuring different critical exponents of the thick films between the critical temperature and the crossover need to be performed. In principle any experiment performed on a bulk three dimensional sample of a critical

fluid mixture can be repeated using a thin film. The possibility of repeating three dimensional experiments in two dimensions is very exciting.

BIBLIOGRAPHY

Bevington, P. R. (1969) Data Reduction and Error Analysis for the Physical Sciences (McGraw-Hill, New York).

Binder, K. (1972) Physica 62, 508.

Birgeneau, R. J., H. J. Guggenheim and G. Shirane (1970) Phys. Rev. B 1, 2211.

Cahn, J. W. (1977) J. Chem. Phys. 66, 3667.

Chen, T. and F. M. Gasparini (1978) Phys. Rev. Lett. 40, 331.

Cox, J. D. and E. F. G. Herington (1956) Trans. Faraday Soc. 52, 928.

Domb, C. (1973) J. Phys. A 6, 1296.

Fisher, M. E. (1971) in Critical Phenomena, International School of Physics "Enrico Fermi," LI Course, 1970, edited by M. S. Green (Academic, New York).

Fisher, M. E. (1973) J. Vac. Sci. Technol. 10, 665.

Greer, S. C. (1976) Phys. Rev. A 14, 1770.

Gülari, E., A. F. Collings, R. L. Schmidt and C. J. Pings (1972) J. Chem. Phys. 56, 6169.

Gutschick, V. P. and C. J. Pings (1971) J. Chem. Phys. 55, 3845.

Handschy, M. A. (1978) private communication.

Ikeda, H. and K. Hirakawa (1974) Solid State Comm. 14, 529.

Jacobs, D. T., R. C. Mockler and W. J. O'Sullivan (1976) Phys. Rev. Lett. 37, 1471.

Jacobs, D. T., D. J. Anthony, R. C. Mockler and W. J. O'Sullivan (1977) Chem. Phys. 20, 219.

Jones, D. C. and S. Amstell (1930) J. Chem. Soc., 1316.

Le Guillou, J. C. and J. Zinn-Justin (1977) Phys. Rev. Lett. 39, 95.

Loven, A. W. and O. K. Rice (1963) Trans. Faraday Soc. 59, 2723.

Lutz, H., J. D. Gunton, H. K. Schurmann, J. E. Crow and T. Mihalisin (1974) Solid State Comm. 14, 1075.

Lyons, K. B., R. C. Mockler and W. J. O'Sullivan (1974) Phys. Rev. A 10, 393.

Shirane, G. and R. J. Birgeneau (1977) Physica 86-88B, 639.

Stanley, H. E. (1971) Introduction to Phase Transitions and Critical Phenomena (Clarendon Press, Oxford).

Stein, A. and G. F. Allen (1973) J. Phys. Chem. Ref. Data 2, 443.

APPENDIX

DATA RUN 1

FILM THICKNESS 2.51 MICRONS

TEMPERATURE (C)	DELTA N
35.0508	0.0486 +/- 0.0008
34.7493	0.0446 +/- 0.0008
34.4594	0.0364 +/- 0.0007
34.2594	0.0313 +/- 0.0007
34.1592	0.0255 +/- 0.0007
34.0892	0.0212 +/- 0.0006
34.0258	0.0136 +/- 0.0006
34.0177	0.0118 +/- 0.0006
34.0133	0.0117 +/- 0.0006
34.0109	0.0100 +/- 0.0006
34.0064	0.0101 +/- 0.0006
34.0001	0.0082 +/- 0.0006
33.9958	0.0070 +/- 0.0006
33.9917	0.0060 +/- 0.0006
33.9886	0.0058 +/- 0.0006

DATA RUN 1

FILM THICKNESS 2.74 MICRONS

TEMPERATURE (C)	DELTA N
35.0508	0.0470 +/- 0.0008
34.7493	0.0427 +/- 0.0008
34.4594	0.0369 +/- 0.0007
34.2594	0.0300 +/- 0.0007
34.1592	0.0254 +/- 0.0007
34.0892	0.0204 +/- 0.0007
34.0492	0.0158 +/- 0.0006
34.0258	0.0130 +/- 0.0006
34.0177	0.0119 +/- 0.0006
34.0133	0.0106 +/- 0.0006
34.0109	0.0095 +/- 0.0006
34.0064	0.0094 +/- 0.0006
34.0001	0.0086 +/- 0.0006
33.9958	0.0077 +/- 0.0006
33.9917	0.0070 +/- 0.0006
33.9886	0.0058 +/- 0.0006

DATA RUN 1

FILM THICKNESS 2.97 MICRONS

TEMPERATURE (C)	DELTA N
35.0508	0.0481 +/- 0.0007
34.7493	0.0424 +/- 0.0007
34.4594	0.0363 +/- 0.0007
34.2594	0.0300 +/- 0.0006
34.1592	0.0254 +/- 0.0006
34.0892	0.0206 +/- 0.0006
34.0492	0.0161 +/- 0.0006
34.0258	0.0132 +/- 0.0005
34.0177	0.0116 +/- 0.0005
34.0133	0.0114 +/- 0.0005
34.0109	0.0094 +/- 0.0005
34.0064	0.0101 +/- 0.0005
34.0001	0.0083 +/- 0.0005
33.9958	0.0075 +/- 0.0005
33.9917	0.0066 +/- 0.0005
33.9886	0.0054 +/- 0.0005

DATA RUN 1

FILM THICKNESS 3.20 MICRONS

TEMPERATURE (C)	DELTA N
34.4594	0.0368 +/- 0.0006
34.2594	0.0314 +/- 0.0006
34.1592	0.0265 +/- 0.0006
34.0892	0.0224 +/- 0.0005
34.0492	0.0178 +/- 0.0005
34.0258	0.0151 +/- 0.0005
34.0177	0.0127 +/- 0.0005
34.0133	0.0137 +/- 0.0005
34.0109	0.0096 +/- 0.0005
34.0064	0.0114 +/- 0.0005
34.0001	0.0100 +/- 0.0005
33.9958	0.0092 +/- 0.0005
33.9917	0.0071 +/- 0.0005
33.9886	0.0050 +/- 0.0004

DATA RUN 2

FILM THICKNESS 2.51 MICRONS

TEMPERATURE (C)	DELTA N
34.9929	0.0461 +/- 0.0008
34.7946	0.0429 +/- 0.0008
34.6234	0.0404 +/- 0.0008
34.4941	0.0364 +/- 0.0008
34.3944	0.0348 +/- 0.0008
34.2999	0.0312 +/- 0.0008
34.2302	0.0289 +/- 0.0007
34.1830	0.0254 +/- 0.0007
34.1567	0.0251 +/- 0.0007
34.1312	0.0232 +/- 0.0007
34.1112	0.0206 +/- 0.0007
34.0940	0.0188 +/- 0.0007
34.0804	0.0183 +/- 0.0007
34.0701	0.0179 +/- 0.0007
34.0649	0.0177 +/- 0.0007
34.0598	0.0170 +/- 0.0007
34.0548	0.0151 +/- 0.0007
34.0510	0.0145 +/- 0.0007
34.0498	0.0140 +/- 0.0007
34.0478	0.0136 +/- 0.0007
34.0471	0.0144 +/- 0.0007
34.0451	0.0136 +/- 0.0007
34.0432	0.0130 +/- 0.0007
34.0412	0.0129 +/- 0.0007
34.0408	0.0127 +/- 0.0007
34.0386	0.0133 +/- 0.0007
34.0380	0.0127 +/- 0.0007
34.0379	0.0136 +/- 0.0007
34.0367	0.0109 +/- 0.0007
34.0367	0.0123 +/- 0.0007
34.0363	0.0126 +/- 0.0007
34.0362	0.0113 +/- 0.0007
34.0337	0.0109 +/- 0.0007
34.0313	0.0111 +/- 0.0007
34.0284	0.0097 +/- 0.0007
34.0263	0.0093 +/- 0.0007
34.0245	0.0089 +/- 0.0006
34.0241	0.0090 +/- 0.0006
34.0234	0.0090 +/- 0.0006
34.0230	0.0069 +/- 0.0006
34.0224	0.0086 +/- 0.0006
34.0220	0.0060 +/- 0.0006
34.0217	0.0074 +/- 0.0006
34.0214	0.0069 +/- 0.0006

DATA RUN 2

FILM THICKNESS 2.74 MICRONS

TEMPERATURE (C)	DELTA N
34.9929	0.0470 +/- 0.0008
34.7946	0.0429 +/- 0.0008
34.6234	0.0398 +/- 0.0008
34.4941	0.0364 +/- 0.0007
34.3944	0.0335 +/- 0.0007
34.2999	0.0314 +/- 0.0007
34.2302	0.0284 +/- 0.0007
34.1830	0.0256 +/- 0.0007
34.1567	0.0242 +/- 0.0007
34.1312	0.0223 +/- 0.0007
34.1112	0.0208 +/- 0.0007
34.1017	0.0198 +/- 0.0007
34.0940	0.0197 +/- 0.0007
34.0940	0.0202 +/- 0.0007
34.0910	0.0194 +/- 0.0007
34.0833	0.0190 +/- 0.0006
34.0804	0.0189 +/- 0.0006
34.0701	0.0172 +/- 0.0006
34.0649	0.0167 +/- 0.0006
34.0598	0.0159 +/- 0.0006
34.0548	0.0149 +/- 0.0006
34.0510	0.0148 +/- 0.0006
34.0498	0.0147 +/- 0.0006
34.0478	0.0141 +/- 0.0006
34.0471	0.0143 +/- 0.0006
34.0451	0.0137 +/- 0.0006
34.0432	0.0129 +/- 0.0006
34.0412	0.0119 +/- 0.0006
34.0408	0.0124 +/- 0.0006
34.0386	0.0117 +/- 0.0006
34.0380	0.0127 +/- 0.0006
34.0379	0.0110 +/- 0.0006
34.0367	0.0108 +/- 0.0006
34.0367	0.0105 +/- 0.0006
34.0363	0.0116 +/- 0.0006
34.0362	0.0110 +/- 0.0006

34.0337	0.0105 +/- 0.0006
34.0313	0.0103 +/- 0.0006
34.0301	0.0099 +/- 0.0006
34.0284	0.0101 +/- 0.0006
34.0263	0.0099 +/- 0.0006
34.0245	0.0096 +/- 0.0006
34.0241	0.0093 +/- 0.0006
34.0234	0.0083 +/- 0.0006
34.0231	0.0089 +/- 0.0006
34.0230	0.0080 +/- 0.0006
34.0224	0.0077 +/- 0.0006
34.0220	0.0079 +/- 0.0006
34.0217	0.0067 +/- 0.0006
34.0214	0.0070 +/- 0.0006

DATA RUN 2

FILM THICKNESS 2.97 MICRONS

TEMPERATURE (C)	DELTA N
34.9929	0.0460 +/- 0.0007
34.7946	0.0425 +/- 0.0007
34.6234	0.0412 +/- 0.0007
34.4941	0.0370 +/- 0.0007
34.3944	0.0331 +/- 0.0006
34.2999	0.0299 +/- 0.0006
34.2302	0.0287 +/- 0.0006
34.1830	0.0253 +/- 0.0006
34.1567	0.0243 +/- 0.0006
34.1312	0.0232 +/- 0.0006
34.1112	0.0214 +/- 0.0006
34.1017	0.0204 +/- 0.0006
34.0940	0.0202 +/- 0.0006
34.0940	0.0189 +/- 0.0006
34.0910	0.0199 +/- 0.0006
34.0833	0.0194 +/- 0.0006
34.0804	0.0177 +/- 0.0006
34.0701	0.0162 +/- 0.0006
34.0649	0.0160 +/- 0.0006
34.0598	0.0164 +/- 0.0006
34.0548	0.0157 +/- 0.0006
34.0510	0.0142 +/- 0.0005
34.0498	0.0154 +/- 0.0006
34.0478	0.0145 +/- 0.0005
34.0471	0.0142 +/- 0.0005
34.0451	0.0128 +/- 0.0005
34.0432	0.0137 +/- 0.0005
34.0412	0.0129 +/- 0.0005
34.0408	0.0133 +/- 0.0005
34.0386	0.0127 +/- 0.0005
34.0380	0.0114 +/- 0.0005
34.0379	0.0121 +/- 0.0005
34.0367	0.0103 +/- 0.0005
34.0367	0.0109 +/- 0.0005
34.0363	0.0110 +/- 0.0005
34.0362	0.0122 +/- 0.0005

34.0337	0.0107 +/- 0.0005
34.0301	0.0107 +/- 0.0005
34.0284	0.0105 +/- 0.0005
34.0263	0.0097 +/- 0.0005
34.0245	0.0104 +/- 0.0005
34.0241	0.0097 +/- 0.0005
34.0234	0.0090 +/- 0.0005
34.0231	0.0090 +/- 0.0005
34.0230	0.0080 +/- 0.0005
34.0224	0.0083 +/- 0.0005
34.0220	0.0081 +/- 0.0005
34.0217	0.0071 +/- 0.0005
34.0214	0.0076 +/- 0.0005
34.0211	0.0066 +/- 0.0005
34.0205	0.0054 +/- 0.0005

DATA RUN 2

FILM THICKNESS 3.20 MICRONS

TEMPERATURE (C)	DELTA N
34.9929	0.0463 +/- 0.0007
34.7946	0.0440 +/- 0.0007
34.6234	0.0442 +/- 0.0007
34.4941	0.0347 +/- 0.0007
34.3944	0.0346 +/- 0.0007
34.2999	0.0317 +/- 0.0007
34.2302	0.0290 +/- 0.0006
34.1830	0.0273 +/- 0.0006
34.1567	0.0258 +/- 0.0006
34.1312	0.0240 +/- 0.0006
34.1112	0.0232 +/- 0.0006
34.1017	0.0229 +/- 0.0006
34.0940	0.0213 +/- 0.0006
34.0940	0.0223 +/- 0.0006
34.0910	0.0220 +/- 0.0006
34.0833	0.0208 +/- 0.0006
34.0804	0.0187 +/- 0.0006
34.0701	0.0183 +/- 0.0006
34.0649	0.0176 +/- 0.0006
34.0598	0.0171 +/- 0.0006
34.0548	0.0159 +/- 0.0006
34.0510	0.0165 +/- 0.0006
34.0498	0.0174 +/- 0.0006
34.0478	0.0168 +/- 0.0006
34.0471	0.0167 +/- 0.0006
34.0451	0.0170 +/- 0.0006
34.0432	0.0146 +/- 0.0006
34.0412	0.0140 +/- 0.0006
34.0408	0.0136 +/- 0.0006
34.0386	0.0144 +/- 0.0006
34.0380	0.0131 +/- 0.0006
34.0379	0.0140 +/- 0.0006
34.0367	0.0146 +/- 0.0006
34.0367	0.0107 +/- 0.0005
34.0363	0.0137 +/- 0.0006
34.0362	0.0139 +/- 0.0006

34.0337	0.0147 +/- 0.0006
34.0313	0.0128 +/- 0.0006
34.0301	0.0137 +/- 0.0006
34.0284	0.0121 +/- 0.0006
34.0263	0.0112 +/- 0.0006
34.0245	0.0118 +/- 0.0006
34.0241	0.0118 +/- 0.0006
34.0234	0.0114 +/- 0.0006
34.0231	0.0125 +/- 0.0006
34.0230	0.0127 +/- 0.0006
34.0224	0.0106 +/- 0.0005
34.0220	0.0112 +/- 0.0006
34.0217	0.0100 +/- 0.0005
34.0214	0.0096 +/- 0.0005
34.0211	0.0097 +/- 0.0005
34.0205	0.0096 +/- 0.0005

DATA RUN 3

FILM THICKNESS 1.83 MICRONS

TEMPERATURE (C)	DELTA N
34.9881	0.0472 +/- 0.0010
34.7887	0.0436 +/- 0.0010
34.5889	0.0390 +/- 0.0010
34.2700	0.0294 +/- 0.0009
34.2716	0.0312 +/- 0.0010
34.2214	0.0272 +/- 0.0009
34.1765	0.0262 +/- 0.0009
34.1463	0.0228 +/- 0.0009
34.1265	0.0229 +/- 0.0009
34.1068	0.0220 +/- 0.0009
34.0915	0.0203 +/- 0.0009
34.0785	0.0184 +/- 0.0009
34.0684	0.0177 +/- 0.0009
34.0614	0.0173 +/- 0.0009
34.0614	0.0169 +/- 0.0009
34.0547	0.0143 +/- 0.0009
34.0502	0.0165 +/- 0.0009
34.0463	0.0160 +/- 0.0009
34.0428	0.0144 +/- 0.0009
34.0395	0.0133 +/- 0.0009
34.0368	0.0132 +/- 0.0009
34.0336	0.0127 +/- 0.0009
34.0309	0.0123 +/- 0.0009
34.0284	0.0118 +/- 0.0009
34.0261	0.0114 +/- 0.0009
34.0235	0.0119 +/- 0.0009
34.0214	0.0118 +/- 0.0009
34.0198	0.0102 +/- 0.0008
34.0186	0.0090 +/- 0.0008
34.0175	0.0089 +/- 0.0008
34.0164	0.0072 +/- 0.0008
34.0156	0.0084 +/- 0.0008
34.0148	0.0102 +/- 0.0008
34.0148	0.0106 +/- 0.0009
34.0132	0.0104 +/- 0.0009
34.0124	0.0088 +/- 0.0008
34.0103	0.0076 +/- 0.0008
34.0082	0.0060 +/- 0.0008

DATA RUN 3

FILM THICKNESS 2.06 MICRONS

TEMPERATURE (C)	DELTA N
34.9881	0.0474 +/- 0.0009
34.7887	0.0436 +/- 0.0009
34.5889	0.0399 +/- 0.0009
34.4390	0.0358 +/- 0.0008
34.3390	0.0328 +/- 0.0008
34.2700	0.0308 +/- 0.0008
34.2716	0.0306 +/- 0.0008
34.2214	0.0275 +/- 0.0008
34.1765	0.0254 +/- 0.0008
34.1463	0.0233 +/- 0.0008
34.1265	0.0225 +/- 0.0008
34.1068	0.0198 +/- 0.0008
34.0915	0.0195 +/- 0.0008
34.0785	0.0178 +/- 0.0007
34.0684	0.0167 +/- 0.0007
34.0614	0.0164 +/- 0.0007
34.0614	0.0164 +/- 0.0007
34.0547	0.0158 +/- 0.0007
34.0502	0.0147 +/- 0.0007
34.0463	0.0146 +/- 0.0007
34.0428	0.0123 +/- 0.0007
34.0395	0.0125 +/- 0.0007
34.0368	0.0128 +/- 0.0007
34.0336	0.0128 +/- 0.0007
34.0309	0.0111 +/- 0.0007
34.0284	0.0100 +/- 0.0007
34.0261	0.0107 +/- 0.0007
34.0235	0.0105 +/- 0.0007
34.0214	0.0093 +/- 0.0007
34.0198	0.0089 +/- 0.0007
34.0186	0.0074 +/- 0.0007
34.0175	0.0068 +/- 0.0007
34.0164	0.0070 +/- 0.0007
34.0156	0.0068 +/- 0.0007
34.0148	0.0058 +/- 0.0007
34.0148	0.0060 +/- 0.0007
34.0143	0.0083 +/- 0.0007
34.0134	0.0079 +/- 0.0007
34.0126	0.0056 +/- 0.0007
34.0126	0.0048 +/- 0.0007

DATA RUN 3

FILM THICKNESS 2.28 MICRONS

TEMPERATURE (C)	DELTA N
34.9881	0.0456 +/- 0.0008
34.7887	0.0423 +/- 0.0008
34.5889	0.0376 +/- 0.0008
34.4390	0.0351 +/- 0.0008
34.2700	0.0288 +/- 0.0008
34.2716	0.0307 +/- 0.0008
34.2214	0.0275 +/- 0.0008
34.1765	0.0248 +/- 0.0007
34.1463	0.0231 +/- 0.0007
34.1265	0.0211 +/- 0.0007
34.1068	0.0197 +/- 0.0007
34.0915	0.0187 +/- 0.0007
34.0785	0.0170 +/- 0.0007
34.0684	0.0167 +/- 0.0007
34.0614	0.0154 +/- 0.0007
34.0614	0.0155 +/- 0.0007
34.0547	0.0150 +/- 0.0007
34.0502	0.0143 +/- 0.0007
34.0463	0.0139 +/- 0.0007
34.0428	0.0139 +/- 0.0007
34.0395	0.0125 +/- 0.0007
34.0368	0.0123 +/- 0.0007
34.0336	0.0122 +/- 0.0007
34.0309	0.0118 +/- 0.0007
34.0284	0.0111 +/- 0.0007
34.0261	0.0107 +/- 0.0007
34.0235	0.0107 +/- 0.0007
34.0214	0.0095 +/- 0.0007
34.0198	0.0086 +/- 0.0007
34.0186	0.0081 +/- 0.0007
34.0175	0.0074 +/- 0.0007
34.0164	0.0072 +/- 0.0007
34.0156	0.0069 +/- 0.0006
34.0148	0.0062 +/- 0.0006
34.0148	0.0063 +/- 0.0006
34.0143	0.0090 +/- 0.0007
34.0134	0.0078 +/- 0.0007
34.0126	0.0068 +/- 0.0006
34.0126	0.0068 +/- 0.0006

DATA RUN 3

FILM THICKNESS 2.51 MICRONS

TEMPERATURE (C)	DELTA N
34.9881	0.0459 +/- 0.0008
34.7887	0.0417 +/- 0.0008
34.5889	0.0391 +/- 0.0008
34.4390	0.0346 +/- 0.0008
34.3390	0.0324 +/- 0.0007
34.2700	0.0279 +/- 0.0007
34.2716	0.0294 +/- 0.0007
34.2214	0.0275 +/- 0.0007
34.1765	0.0250 +/- 0.0007
34.1463	0.0229 +/- 0.0007
34.1265	0.0218 +/- 0.0007
34.1068	0.0209 +/- 0.0007
34.0915	0.0194 +/- 0.0007
34.0785	0.0182 +/- 0.0007
34.0684	0.0175 +/- 0.0007
34.0614	0.0167 +/- 0.0007
34.0614	0.0165 +/- 0.0007
34.0547	0.0151 +/- 0.0007
34.0502	0.0148 +/- 0.0007
34.0463	0.0143 +/- 0.0007
34.0428	0.0138 +/- 0.0007
34.0395	0.0138 +/- 0.0007
34.0368	0.0133 +/- 0.0006
34.0336	0.0127 +/- 0.0006
34.0309	0.0128 +/- 0.0006
34.0284	0.0112 +/- 0.0006
34.0261	0.0114 +/- 0.0006
34.0235	0.0117 +/- 0.0006
34.0214	0.0094 +/- 0.0006
34.0198	0.0075 +/- 0.0006
34.0186	0.0084 +/- 0.0006
34.0175	0.0082 +/- 0.0006
34.0164	0.0081 +/- 0.0006
34.0156	0.0077 +/- 0.0006
34.0148	0.0069 +/- 0.0006
34.0148	0.0073 +/- 0.0006
34.0143	0.0097 +/- 0.0006
34.0134	0.0093 +/- 0.0006
34.0126	0.0087 +/- 0.0006
34.0126	0.0096 +/- 0.0006
34.0105	0.0071 +/- 0.0006
34.0084	0.0051 +/- 0.0006

DATA RUN 3

FILM THICKNESS 2.74 MICRONS

TEMPERATURE (C)	DELTA N
34.9881	0.0468 +/- 0.0008
34.7887	0.0423 +/- 0.0008
34.5889	0.0391 +/- 0.0007
34.4390	0.0358 +/- 0.0007
34.3390	0.0327 +/- 0.0007
34.2700	0.0300 +/- 0.0007
34.2716	0.0296 +/- 0.0007
34.2214	0.0283 +/- 0.0007
34.1765	0.0261 +/- 0.0007
34.1463	0.0244 +/- 0.0007
34.1265	0.0229 +/- 0.0007
34.1068	0.0214 +/- 0.0007
34.0915	0.0202 +/- 0.0007
34.0785	0.0193 +/- 0.0007
34.0684	0.0178 +/- 0.0006
34.0614	0.0172 +/- 0.0006
34.0614	0.0169 +/- 0.0006
34.0547	0.0176 +/- 0.0006
34.0502	0.0164 +/- 0.0006
34.0463	0.0155 +/- 0.0006
34.0428	0.0151 +/- 0.0006
34.0395	0.0147 +/- 0.0006
34.0368	0.0145 +/- 0.0006
34.0336	0.0134 +/- 0.0006
34.0309	0.0127 +/- 0.0006
34.0284	0.0121 +/- 0.0006
34.0261	0.0118 +/- 0.0006
34.0235	0.0105 +/- 0.0006
34.0214	0.0115 +/- 0.0006
34.0198	0.0103 +/- 0.0006
34.0186	0.0099 +/- 0.0006
34.0175	0.0095 +/- 0.0006
34.0164	0.0105 +/- 0.0006
34.0156	0.0089 +/- 0.0006
34.0148	0.0093 +/- 0.0006
34.0148	0.0093 +/- 0.0006
34.0143	0.0133 +/- 0.0006
34.0134	0.0119 +/- 0.0006
34.0126	0.0119 +/- 0.0006
34.0126	0.0104 +/- 0.0006
34.0105	0.0103 +/- 0.0006
34.0084	0.0101 +/- 0.0006

DATA RUN 4

FILM THICKNESS 0.69 MICRONS

TEMPERATURE (C)	DELTA N
34.9992	0.0495 +/- 0.0015
34.7073	0.0421 +/- 0.0015
34.4972	0.0365 +/- 0.0014
34.3489	0.0343 +/- 0.0014
34.2574	0.0293 +/- 0.0014
34.1525	0.0279 +/- 0.0014
34.1331	0.0239 +/- 0.0014
34.1185	0.0173 +/- 0.0013
34.1064	0.0188 +/- 0.0013
34.0970	0.0184 +/- 0.0013
34.0878	0.0188 +/- 0.0013
34.0808	0.0186 +/- 0.0013
34.0758	0.0177 +/- 0.0013
34.0721	0.0152 +/- 0.0013
34.0697	0.0163 +/- 0.0013
34.0664	0.0142 +/- 0.0013
34.0622	0.0144 +/- 0.0013
34.0585	0.0146 +/- 0.0013
34.0550	0.0131 +/- 0.0013
34.0523	0.0119 +/- 0.0013
34.0497	0.0167 +/- 0.0013
34.0374	0.0109 +/- 0.0013
34.0248	0.0111 +/- 0.0013
34.0201	0.0091 +/- 0.0013

DATA RUN 4

FILM THICKNESS 0.91 MICRONS

TEMPERATURE (C)	DELTA N
34.9992	0.0489 +/- 0.0012
34.7073	0.0377 +/- 0.0011
34.4972	0.0384 +/- 0.0011
34.3489	0.0311 +/- 0.0011
34.2574	0.0269 +/- 0.0011
34.1928	0.0235 +/- 0.0011
34.1525	0.0208 +/- 0.0011
34.1331	0.0190 +/- 0.0010
34.1185	0.0186 +/- 0.0010
34.1064	0.0181 +/- 0.0010
34.0970	0.0170 +/- 0.0010
34.0878	0.0161 +/- 0.0010
34.0808	0.0151 +/- 0.0010
34.0758	0.0147 +/- 0.0010
34.0721	0.0142 +/- 0.0010
34.0697	0.0140 +/- 0.0010
34.0664	0.0134 +/- 0.0010
34.0622	0.0132 +/- 0.0010
34.0585	0.0127 +/- 0.0010
34.0550	0.0126 +/- 0.0010
34.0523	0.0127 +/- 0.0010
34.0497	0.0119 +/- 0.0010
34.0471	0.0112 +/- 0.0010
34.0445	0.0111 +/- 0.0010
34.0420	0.0104 +/- 0.0010
34.0397	0.0108 +/- 0.0010
34.0374	0.0113 +/- 0.0010
34.0358	0.0110 +/- 0.0010
34.0344	0.0107 +/- 0.0010
34.0328	0.0117 +/- 0.0010
34.0314	0.0110 +/- 0.0010
34.0303	0.0105 +/- 0.0010
34.0292	0.0105 +/- 0.0010

34.0270	0.0104 +/- 0.0010
34.0248	0.0102 +/- 0.0010
34.0232	0.0104 +/- 0.0010
34.0220	0.0093 +/- 0.0010
34.0210	0.0095 +/- 0.0010
34.0201	0.0090 +/- 0.0010
34.0194	0.0097 +/- 0.0010
34.0193	0.0086 +/- 0.0010
34.0190	0.0079 +/- 0.0010
34.0188	0.0086 +/- 0.0010
34.0184	0.0084 +/- 0.0010
34.0182	0.0094 +/- 0.0010
34.0180	0.0081 +/- 0.0010
34.0178	0.0079 +/- 0.0010
34.0174	0.0072 +/- 0.0010

DATA RUN 4

FILM THICKNESS 1.14 MICRONS

TEMPERATURE (C)	DELTA N
34.9992	0.0470 +/- 0.0011
34.7073	0.0399 +/- 0.0010
34.4972	0.0387 +/- 0.0010
34.3489	0.0323 +/- 0.0010
34.2574	0.0276 +/- 0.0010
34.1928	0.0266 +/- 0.0010
34.1525	0.0246 +/- 0.0010
34.1331	0.0239 +/- 0.0010
34.1185	0.0202 +/- 0.0009
34.1064	0.0192 +/- 0.0009
34.0970	0.0204 +/- 0.0009
34.0878	0.0175 +/- 0.0009
34.0808	0.0157 +/- 0.0009
34.0758	0.0157 +/- 0.0009
34.0721	0.0168 +/- 0.0009
34.0697	0.0173 +/- 0.0009
34.0664	0.0166 +/- 0.0009
34.0622	0.0145 +/- 0.0009
34.0585	0.0151 +/- 0.0009
34.0550	0.0161 +/- 0.0009
34.0523	0.0143 +/- 0.0009
34.0497	0.0147 +/- 0.0009
34.0471	0.0134 +/- 0.0009
34.0445	0.0127 +/- 0.0009
34.0420	0.0133 +/- 0.0009
34.0374	0.0120 +/- 0.0009
34.0358	0.0111 +/- 0.0009
34.0344	0.0112 +/- 0.0009
34.0328	0.0117 +/- 0.0009
34.0314	0.0112 +/- 0.0009
34.0303	0.0107 +/- 0.0009
34.0292	0.0101 +/- 0.0009

34.0270	0.0106 +/- 0.0009
34.0248	0.0100 +/- 0.0009
34.0232	0.0096 +/- 0.0009
34.0220	0.0095 +/- 0.0009
34.0210	0.0086 +/- 0.0009
34.0201	0.0097 +/- 0.0009
34.0193	0.0098 +/- 0.0009
34.0190	0.0082 +/- 0.0009
34.0188	0.0078 +/- 0.0009
34.0184	0.0091 +/- 0.0009
34.0182	0.0084 +/- 0.0009
34.0182	0.0079 +/- 0.0009
34.0178	0.0090 +/- 0.0009
34.0174	0.0077 +/- 0.0009
34.0164	0.0083 +/- 0.0009
34.0155	0.0074 +/- 0.0009
34.0131	0.0062 +/- 0.0009
34.0131	0.0063 +/- 0.0009

DATA RUN 5

FILM THICKNESS 5.25 MICRONS

TEMPERATURE (C)	DELTA N
34.1377	0.0247 +/- 0.0003
34.0643	0.0188 +/- 0.0003
34.0336	0.0161 +/- 0.0003
34.0162	0.0126 +/- 0.0003
34.0108	0.0111 +/- 0.0003
34.0082	0.0099 +/- 0.0003
34.0067	0.0098 +/- 0.0003
34.0042	0.0086 +/- 0.0003
34.0026	0.0083 +/- 0.0003
34.0020	0.0082 +/- 0.0003
34.0012	0.0074 +/- 0.0003
34.0003	0.0077 +/- 0.0003
34.0000	0.0065 +/- 0.0003
33.9997	0.0062 +/- 0.0003
33.9994	0.0067 +/- 0.0003
33.9989	0.0059 +/- 0.0003
33.9986	0.0065 +/- 0.0003
33.9984	0.0060 +/- 0.0003
33.9970	0.0055 +/- 0.0003
33.9985	0.0057 +/- 0.0003
33.9980	0.0057 +/- 0.0003
33.9980	0.0055 +/- 0.0003
33.9976	0.0052 +/- 0.0003
33.9975	0.0055 +/- 0.0003
33.9974	0.0046 +/- 0.0002
33.9974	0.0055 +/- 0.0003
33.9974	0.0049 +/- 0.0003
33.9971	0.0058 +/- 0.0003
33.9969	0.0042 +/- 0.0002
33.9969	0.0054 +/- 0.0003
33.9967	0.0051 +/- 0.0003
33.9967	0.0051 +/- 0.0003
33.9966	0.0050 +/- 0.0003
33.9965	0.0037 +/- 0.0002
33.9965	0.0048 +/- 0.0003
33.9965	0.0046 +/- 0.0002
33.9963	0.0046 +/- 0.0002
33.9962	0.0033 +/- 0.0002
33.9962	0.0039 +/- 0.0002
33.9961	0.0038 +/- 0.0002

DATA RUN 5

FILM THICKNESS 5.48 MICRONS

TEMPERATURE (C)	DELTA N
34.1377	0.0240 +/- 0.0003
34.0643	0.0189 +/- 0.0003
34.0336	0.0154 +/- 0.0003
34.0162	0.0121 +/- 0.0003
34.0108	0.0105 +/- 0.0003
34.0082	0.0098 +/- 0.0003
34.0067	0.0096 +/- 0.0003
34.0042	0.0088 +/- 0.0003
34.0026	0.0076 +/- 0.0003
34.0020	0.0079 +/- 0.0003
34.0012	0.0073 +/- 0.0003
34.0003	0.0073 +/- 0.0003
34.0000	0.0067 +/- 0.0003
33.9997	0.0067 +/- 0.0002
33.9994	0.0065 +/- 0.0002
33.9989	0.0059 +/- 0.0002
33.9986	0.0067 +/- 0.0002
33.9984	0.0057 +/- 0.0002
33.9970	0.0056 +/- 0.0002
33.9985	0.0058 +/- 0.0002
33.9980	0.0062 +/- 0.0002
33.9980	0.0055 +/- 0.0002
33.9976	0.0057 +/- 0.0002
33.9975	0.0056 +/- 0.0002
33.9974	0.0048 +/- 0.0002
33.9974	0.0048 +/- 0.0002
33.9974	0.0053 +/- 0.0002
33.9971	0.0053 +/- 0.0002
33.9969	0.0041 +/- 0.0002
33.9969	0.0053 +/- 0.0002
33.9967	0.0052 +/- 0.0002
33.9967	0.0050 +/- 0.0002
33.9966	0.0048 +/- 0.0002
33.9965	0.0039 +/- 0.0002
33.9965	0.0051 +/- 0.0002
33.9965	0.0051 +/- 0.0002
33.9963	0.0045 +/- 0.0002
33.9962	0.0035 +/- 0.0002
33.9962	0.0045 +/- 0.0002
33.9961	0.0039 +/- 0.0002

DATA RUN 5

FILM THICKNESS 5.71 MICRONS

TEMPERATURE (C)	DELTA N
34.1377	0.0239 +/- 0.0003
34.0643	0.0188 +/- 0.0003
34.0336	0.0148 +/- 0.0003
34.0162	0.0122 +/- 0.0003
34.0108	0.0108 +/- 0.0003
34.0082	0.0102 +/- 0.0003
34.0067	0.0094 +/- 0.0003
34.0042	0.0093 +/- 0.0003
34.0026	0.0079 +/- 0.0002
34.0020	0.0080 +/- 0.0002
34.0012	0.0069 +/- 0.0002
34.0003	0.0075 +/- 0.0002
34.0000	0.0067 +/- 0.0002
33.9997	0.0064 +/- 0.0002
33.9994	0.0066 +/- 0.0002
33.9989	0.0064 +/- 0.0002
33.9986	0.0067 +/- 0.0002
33.9984	0.0059 +/- 0.0002
33.9970	0.0061 +/- 0.0002
33.9985	0.0053 +/- 0.0002
33.9980	0.0061 +/- 0.0002
33.9980	0.0057 +/- 0.0002
33.9976	0.0061 +/- 0.0002
33.9975	0.0060 +/- 0.0002
33.9974	0.0046 +/- 0.0002
33.9974	0.0052 +/- 0.0002
33.9974	0.0061 +/- 0.0002
33.9971	0.0053 +/- 0.0002
33.9969	0.0044 +/- 0.0002
33.9969	0.0055 +/- 0.0002
33.9967	0.0055 +/- 0.0002
33.9967	0.0051 +/- 0.0002
33.9966	0.0053 +/- 0.0002
33.9965	0.0041 +/- 0.0002
33.9965	0.0049 +/- 0.0002
33.9965	0.0053 +/- 0.0002
33.9963	0.0044 +/- 0.0002
33.9962	0.0034 +/- 0.0002
33.9962	0.0046 +/- 0.0002
33.9961	0.0047 +/- 0.0002

DATA RUN 6

FILM THICKNESS 14.39 MICRONS

TEMPERATURE (C)	DELTA N
34.0082	0.0129 +/- 0.0001
34.0063	0.0131 +/- 0.0001
34.0041	0.0117 +/- 0.0001
34.0011	0.0108 +/- 0.0001
33.9983	0.0101 +/- 0.0001
33.9948	0.0085 +/- 0.0001
33.9920	0.0063 +/- 0.0001
33.9907	0.0055 +/- 0.0001
33.9899	0.0043 +/- 0.0001
33.9896	0.0017 +/- 0.0001
33.9890	0.0014 +/- 0.0001
33.9890	0.0014 +/- 0.0001
33.9890	0.0014 +/- 0.0001
33.9890	0.0014 +/- 0.0001
33.9890	0.0014 +/- 0.0001
33.9890	0.0014 +/- 0.0001

DATA RUN 6

FILM THICKNESS 14.62 MICRONS

TEMPERATURE (C)	DELTA N
34.0082	0.0124 +/- 0.0002
34.0063	0.0119 +/- 0.0002
34.0041	0.0110 +/- 0.0002
34.0011	0.0106 +/- 0.0002
33.9983	0.0091 +/- 0.0002
33.9948	0.0085 +/- 0.0002
33.9920	0.0066 +/- 0.0002
33.9907	0.0056 +/- 0.0002
33.9899	0.0047 +/- 0.0002
33.9896	0.0019 +/- 0.0001
33.9890	0.0014 +/- 0.0001
33.9890	0.0014 +/- 0.0001
33.9890	0.0014 +/- 0.0001
33.9890	0.0014 +/- 0.0001
33.9890	0.0014 +/- 0.0001
33.9890	0.0014 +/- 0.0001

DATA RUN 6

FILM THICKNESS 14.85 MICRONS

TEMPERATURE (C)	DELTA N
34.0082	0.0127 +/- 0.0002
34.0063	0.0124 +/- 0.0002
34.0041	0.0118 +/- 0.0002
34.0011	0.0106 +/- 0.0002
33.9983	0.0095 +/- 0.0002
33.9948	0.0083 +/- 0.0002
33.9920	0.0063 +/- 0.0002
33.9907	0.0054 +/- 0.0002
33.9899	0.0044 +/- 0.0002
33.9896	0.0017 +/- 0.0002
33.9890	0.0014 +/- 0.0002
33.9890	0.0014 +/- 0.0002
33.9890	0.0014 +/- 0.0002
33.9890	0.0014 +/- 0.0002
33.9890	0.0014 +/- 0.0002
33.9890	0.0014 +/- 0.0002

DATA RUN 7

FILM THICKNESS 1.37 MICRONS

TEMPERATURE (C)	DELTA N
35.0658	0.0489 +/- 0.0009
35.0658	0.0477 +/- 0.0009
34.9051	0.0447 +/- 0.0008
34.7752	0.0438 +/- 0.0008
34.6753	0.0410 +/- 0.0008
34.5707	0.0398 +/- 0.0008
34.4738	0.0370 +/- 0.0008
34.3735	0.0342 +/- 0.0008
34.2883	0.0319 +/- 0.0008
34.2115	0.0281 +/- 0.0008
34.1621	0.0255 +/- 0.0007
34.1293	0.0247 +/- 0.0007
34.1059	0.0229 +/- 0.0007
34.0911	0.0205 +/- 0.0007
34.0808	0.0195 +/- 0.0007
34.0767	0.0197 +/- 0.0007
34.0739	0.0184 +/- 0.0007
34.0673	0.0185 +/- 0.0007
34.0657	0.0191 +/- 0.0007
34.0605	0.0166 +/- 0.0007
34.0598	0.0168 +/- 0.0007
34.0536	0.0155 +/- 0.0007
34.0506	0.0168 +/- 0.0007
34.0487	0.0155 +/- 0.0007
34.0433	0.0158 +/- 0.0007
34.0405	0.0147 +/- 0.0007
34.0396	0.0154 +/- 0.0007
34.0365	0.0158 +/- 0.0007
34.0343	0.0157 +/- 0.0007
34.0324	0.0149 +/- 0.0007
34.0300	0.0146 +/- 0.0007
34.0278	0.0139 +/- 0.0007

34.0252	0.0132 +/- 0.0007
34.0233	0.0137 +/- 0.0007
34.0217	0.0133 +/- 0.0007
34.0201	0.0127 +/- 0.0007
34.0181	0.0124 +/- 0.0007
34.0167	0.0124 +/- 0.0007
34.0148	0.0102 +/- 0.0007
34.0137	0.0094 +/- 0.0007
34.0123	0.0098 +/- 0.0007
34.0107	0.0100 +/- 0.0007
34.0100	0.0089 +/- 0.0007
34.0090	0.0081 +/- 0.0007
34.0088	0.0084 +/- 0.0007
34.0079	0.0087 +/- 0.0007
34.0068	0.0078 +/- 0.0007
34.0061	0.0075 +/- 0.0007
34.0053	0.0075 +/- 0.0007
34.0040	0.0059 +/- 0.0006
34.0025	0.0071 +/- 0.0007
34.0018	0.0038 +/- 0.0006
34.0014	0.0037 +/- 0.0006

DATA RUN 7

FILM THICKNESS 1.60 MICRONS

TEMPERATURE (C)	DELTA N
35.0658	0.0461 +/- 0.0007
35.0658	0.0466 +/- 0.0007
34.9051	0.0446 +/- 0.0007
34.7752	0.0423 +/- 0.0007
34.6753	0.0405 +/- 0.0007
34.5707	0.0378 +/- 0.0007
34.4738	0.0350 +/- 0.0007
34.3735	0.0325 +/- 0.0007
34.2883	0.0299 +/- 0.0007
34.2115	0.0263 +/- 0.0006
34.1621	0.0235 +/- 0.0006
34.1293	0.0218 +/- 0.0006
34.1059	0.0200 +/- 0.0006
34.0911	0.0179 +/- 0.0006
34.0808	0.0177 +/- 0.0006
34.0767	0.0163 +/- 0.0006
34.0739	0.0166 +/- 0.0006
34.0673	0.0161 +/- 0.0006
34.0657	0.0165 +/- 0.0006
34.0605	0.0164 +/- 0.0006
34.0598	0.0154 +/- 0.0006
34.0536	0.0150 +/- 0.0006
34.0506	0.0144 +/- 0.0006
34.0487	0.0143 +/- 0.0006
34.0433	0.0138 +/- 0.0006
34.0405	0.0128 +/- 0.0006
34.0396	0.0133 +/- 0.0006
34.0365	0.0129 +/- 0.0006
34.0343	0.0133 +/- 0.0006
34.0324	0.0123 +/- 0.0006
34.0300	0.0120 +/- 0.0006
34.0278	0.0115 +/- 0.0006

34.0252	0.0113 +/- 0.0006
34.0233	0.0105 +/- 0.0006
34.0217	0.0101 +/- 0.0006
34.0201	0.0093 +/- 0.0006
34.0181	0.0092 +/- 0.0006
34.0167	0.0097 +/- 0.0006
34.0148	0.0088 +/- 0.0006
34.0137	0.0087 +/- 0.0006
34.0123	0.0083 +/- 0.0006
34.0107	0.0078 +/- 0.0006
34.0100	0.0073 +/- 0.0006
34.0090	0.0075 +/- 0.0006
34.0088	0.0069 +/- 0.0006
34.0079	0.0065 +/- 0.0005
34.0068	0.0066 +/- 0.0005
34.0061	0.0067 +/- 0.0005
34.0053	0.0059 +/- 0.0005
34.0040	0.0053 +/- 0.0005
34.0031	0.0050 +/- 0.0005
34.0025	0.0046 +/- 0.0005
34.0020	0.0038 +/- 0.0005
34.0018	0.0038 +/- 0.0005
34.0014	0.0046 +/- 0.0005

DATA RUN 7

FILM THICKNESS 1.83 MICRONS

TEMPERATURE (C)	DELTA N
35.0658	0.0469 +/- 0.0007
35.0658	0.0449 +/- 0.0007
34.9051	0.0435 +/- 0.0007
34.7752	0.0417 +/- 0.0007
34.6753	0.0409 +/- 0.0007
34.5707	0.0389 +/- 0.0007
34.3735	0.0331 +/- 0.0006
34.2883	0.0301 +/- 0.0006
34.2115	0.0296 +/- 0.0006
34.1621	0.0248 +/- 0.0006
34.1293	0.0227 +/- 0.0006
34.1059	0.0211 +/- 0.0006
34.0808	0.0183 +/- 0.0006
34.0767	0.0197 +/- 0.0006
34.0739	0.0182 +/- 0.0006
34.0673	0.0181 +/- 0.0006
34.0657	0.0174 +/- 0.0006
34.0605	0.0169 +/- 0.0006
34.0598	0.0176 +/- 0.0006
34.0536	0.0174 +/- 0.0006
34.0506	0.0159 +/- 0.0006
34.0487	0.0153 +/- 0.0006
34.0433	0.0150 +/- 0.0006
34.0405	0.0146 +/- 0.0006
34.0396	0.0142 +/- 0.0006
34.0365	0.0141 +/- 0.0006
34.0343	0.0137 +/- 0.0006
34.0324	0.0134 +/- 0.0006
34.0300	0.0133 +/- 0.0005
34.0278	0.0129 +/- 0.0005
34.0252	0.0121 +/- 0.0005
34.0233	0.0112 +/- 0.0005

34.0217	0.0108 +/- 0.0005
34.0201	0.0104 +/- 0.0005
34.0181	0.0098 +/- 0.0005
34.0167	0.0098 +/- 0.0005
34.0148	0.0095 +/- 0.0005
34.0137	0.0090 +/- 0.0005
34.0123	0.0081 +/- 0.0005
34.0107	0.0080 +/- 0.0005
34.0100	0.0081 +/- 0.0005
34.0090	0.0076 +/- 0.0005
34.0088	0.0072 +/- 0.0005
34.0079	0.0077 +/- 0.0005
34.0068	0.0074 +/- 0.0005
34.0061	0.0071 +/- 0.0005
34.0053	0.0054 +/- 0.0005
34.0040	0.0050 +/- 0.0005
34.0031	0.0045 +/- 0.0005
34.0025	0.0054 +/- 0.0005
34.0020	0.0054 +/- 0.0005
34.0018	0.0050 +/- 0.0005
34.0014	0.0059 +/- 0.0005

DATA RUN 8

FILM THICKNESS 3.66 MICRONS

TEMPERATURE (C)	DELTA N
34.2745	0.0312 +/- 0.0004
34.2339	0.0297 +/- 0.0004
34.2025	0.0281 +/- 0.0004
34.1656	0.0259 +/- 0.0004
34.1354	0.0249 +/- 0.0004
34.1105	0.0230 +/- 0.0004
34.0912	0.0212 +/- 0.0004
34.0767	0.0200 +/- 0.0004
34.0664	0.0190 +/- 0.0004
34.0585	0.0186 +/- 0.0004
34.0505	0.0177 +/- 0.0003
34.0443	0.0174 +/- 0.0003
34.0390	0.0164 +/- 0.0003
34.0340	0.0158 +/- 0.0003
34.0293	0.0147 +/- 0.0003
34.0252	0.0144 +/- 0.0003
34.0210	0.0138 +/- 0.0003
34.0170	0.0124 +/- 0.0003
34.0140	0.0121 +/- 0.0003
34.0131	0.0116 +/- 0.0003
34.0118	0.0120 +/- 0.0003
34.0098	0.0113 +/- 0.0003
34.0084	0.0109 +/- 0.0003
34.0077	0.0102 +/- 0.0003
34.0064	0.0099 +/- 0.0003
34.0058	0.0097 +/- 0.0003
34.0053	0.0096 +/- 0.0003
34.0052	0.0096 +/- 0.0003
34.0047	0.0088 +/- 0.0003
34.0045	0.0087 +/- 0.0003
34.0043	0.0088 +/- 0.0003
34.0040	0.0088 +/- 0.0003
34.0039	0.0089 +/- 0.0003
34.0036	0.0085 +/- 0.0003
34.0034	0.0077 +/- 0.0003
34.0028	0.0078 +/- 0.0003
34.0024	0.0074 +/- 0.0003
34.0022	0.0076 +/- 0.0003

34.0020	0.0074 +/- 0.0003
34.0019	0.0072 +/- 0.0003
34.0019	0.0074 +/- 0.0003
34.0016	0.0070 +/- 0.0003
34.0016	0.0074 +/- 0.0003
34.0015	0.0069 +/- 0.0003
34.0013	0.0066 +/- 0.0003
34.0012	0.0065 +/- 0.0003
34.0009	0.0062 +/- 0.0003
34.0005	0.0054 +/- 0.0003
34.0005	0.0069 +/- 0.0003
34.0002	0.0053 +/- 0.0003
34.0001	0.0062 +/- 0.0003
34.0000	0.0051 +/- 0.0003
33.9997	0.0046 +/- 0.0003
33.9996	0.0059 +/- 0.0003
33.9995	0.0053 +/- 0.0003
33.9994	0.0046 +/- 0.0003
33.9993	0.0057 +/- 0.0003
33.9993	0.0049 +/- 0.0003
33.9992	0.0051 +/- 0.0003
33.9992	0.0048 +/- 0.0003
33.9992	0.0046 +/- 0.0003
33.9990	0.0045 +/- 0.0003
33.9988	0.0040 +/- 0.0003
33.9986	0.0039 +/- 0.0003
33.9985	0.0040 +/- 0.0003
33.9984	0.0038 +/- 0.0003
33.9983	0.0033 +/- 0.0003
33.9982	0.0042 +/- 0.0003
33.9981	0.0032 +/- 0.0003
33.9979	0.0034 +/- 0.0003
33.9977	0.0027 +/- 0.0003
33.9973	0.0028 +/- 0.0003

DATA RUN 8

FILM THICKNESS 3.88 MICRONS

TEMPERATURE (C)	DELTA N
34.2745	0.0312 +/- 0.0004
34.2339	0.0296 +/- 0.0004
34.2025	0.0286 +/- 0.0004
34.1656	0.0258 +/- 0.0004
34.1354	0.0249 +/- 0.0004
34.1105	0.0221 +/- 0.0004
34.0912	0.0211 +/- 0.0003
34.0767	0.0197 +/- 0.0003
34.0664	0.0185 +/- 0.0003
34.0585	0.0177 +/- 0.0003
34.0505	0.0171 +/- 0.0003
34.0443	0.0168 +/- 0.0003
34.0390	0.0152 +/- 0.0003
34.0340	0.0148 +/- 0.0003
34.0293	0.0141 +/- 0.0003
34.0252	0.0133 +/- 0.0003
34.0210	0.0128 +/- 0.0003
34.0170	0.0117 +/- 0.0003
34.0140	0.0113 +/- 0.0003
34.0131	0.0111 +/- 0.0003
34.0118	0.0105 +/- 0.0003
34.0098	0.0100 +/- 0.0003
34.0084	0.0099 +/- 0.0003
34.0077	0.0096 +/- 0.0003
34.0064	0.0091 +/- 0.0003
34.0058	0.0089 +/- 0.0003
34.0053	0.0085 +/- 0.0003
34.0052	0.0085 +/- 0.0003
34.0047	0.0084 +/- 0.0003
34.0045	0.0076 +/- 0.0003
34.0043	0.0083 +/- 0.0003
34.0040	0.0076 +/- 0.0003
34.0039	0.0074 +/- 0.0003
34.0036	0.0076 +/- 0.0003
34.0034	0.0072 +/- 0.0003
34.0028	0.0073 +/- 0.0003
34.0024	0.0067 +/- 0.0003
34.0022	0.0070 +/- 0.0003

34.0020	0.0068 +/- 0.0003
34.0019	0.0066 +/- 0.0003
34.0019	0.0068 +/- 0.0003
34.0016	0.0066 +/- 0.0003
34.0016	0.0071 +/- 0.0003
34.0015	0.0063 +/- 0.0003
34.0013	0.0059 +/- 0.0003
34.0012	0.0060 +/- 0.0003
34.0009	0.0054 +/- 0.0003
34.0005	0.0050 +/- 0.0003
34.0005	0.0051 +/- 0.0003
34.0002	0.0046 +/- 0.0003
34.0001	0.0047 +/- 0.0003
34.0000	0.0045 +/- 0.0003
33.9997	0.0045 +/- 0.0003
33.9996	0.0046 +/- 0.0003
33.9995	0.0052 +/- 0.0003
33.9994	0.0042 +/- 0.0003
33.9993	0.0043 +/- 0.0003
33.9993	0.0046 +/- 0.0003
33.9992	0.0045 +/- 0.0003
33.9992	0.0042 +/- 0.0003
33.9992	0.0039 +/- 0.0003
33.9990	0.0041 +/- 0.0003
33.9988	0.0035 +/- 0.0003
33.9986	0.0031 +/- 0.0003
33.9985	0.0033 +/- 0.0003
33.9984	0.0028 +/- 0.0003
33.9983	0.0029 +/- 0.0003
33.9982	0.0035 +/- 0.0003
33.9981	0.0026 +/- 0.0003
33.9979	0.0019 +/- 0.0003

DATA RUN 8

FILM THICKNESS 4.11 MICRONS

TEMPERATURE (C)	DELTA N
34.2745	0.0302 +/- 0.0004
34.2339	0.0282 +/- 0.0004
34.2025	0.0272 +/- 0.0004
34.1656	0.0253 +/- 0.0004
34.1354	0.0234 +/- 0.0003
34.1105	0.0218 +/- 0.0003
34.0912	0.0203 +/- 0.0003
34.0767	0.0195 +/- 0.0003
34.0664	0.0182 +/- 0.0003
34.0585	0.0174 +/- 0.0003
34.0505	0.0160 +/- 0.0003
34.0443	0.0162 +/- 0.0003
34.0390	0.0155 +/- 0.0003
34.0340	0.0146 +/- 0.0003
34.0293	0.0139 +/- 0.0003
34.0252	0.0129 +/- 0.0003
34.0210	0.0126 +/- 0.0003
34.0170	0.0110 +/- 0.0003
34.0140	0.0109 +/- 0.0003
34.0131	0.0103 +/- 0.0003
34.0118	0.0105 +/- 0.0003
34.0098	0.0098 +/- 0.0003
34.0084	0.0096 +/- 0.0003
34.0077	0.0094 +/- 0.0003
34.0064	0.0090 +/- 0.0003
34.0058	0.0086 +/- 0.0003
34.0053	0.0086 +/- 0.0003
34.0052	0.0083 +/- 0.0003
34.0047	0.0081 +/- 0.0003
34.0045	0.0075 +/- 0.0003
34.0043	0.0078 +/- 0.0003
34.0040	0.0073 +/- 0.0003
34.0039	0.0077 +/- 0.0003
34.0036	0.0075 +/- 0.0003
34.0034	0.0078 +/- 0.0003
34.0028	0.0071 +/- 0.0003
34.0024	0.0073 +/- 0.0003

34.0022	0.0070 +/- 0.0003
34.0020	0.0070 +/- 0.0003
34.0019	0.0067 +/- 0.0003
34.0019	0.0069 +/- 0.0003
34.0016	0.0062 +/- 0.0003
34.0016	0.0066 +/- 0.0003
34.0015	0.0061 +/- 0.0003
34.0013	0.0058 +/- 0.0003
34.0012	0.0061 +/- 0.0003
34.0009	0.0056 +/- 0.0003
34.0005	0.0052 +/- 0.0003
34.0005	0.0052 +/- 0.0003
34.0002	0.0048 +/- 0.0003
34.0001	0.0047 +/- 0.0003
34.0000	0.0045 +/- 0.0003
33.9997	0.0044 +/- 0.0003
33.9996	0.0044 +/- 0.0003
33.9995	0.0049 +/- 0.0003
33.9994	0.0042 +/- 0.0003
33.9993	0.0041 +/- 0.0003
33.9993	0.0046 +/- 0.0003
33.9992	0.0043 +/- 0.0003
33.9992	0.0045 +/- 0.0003
33.9992	0.0039 +/- 0.0003
33.9990	0.0040 +/- 0.0003
33.9988	0.0035 +/- 0.0002
33.9986	0.0033 +/- 0.0002
33.9985	0.0034 +/- 0.0002
33.9984	0.0028 +/- 0.0002
33.9983	0.0029 +/- 0.0002
33.9982	0.0030 +/- 0.0002
33.9981	0.0029 +/- 0.0002
33.9979	0.0024 +/- 0.0002

DATA RUN 8

FILM THICKNESS 4.34 MICRONS

TEMPERATURE (C)	DELTA N
34.2745	0.0314 +/- 0.0004
34.2339	0.0291 +/- 0.0004
34.2025	0.0272 +/- 0.0004
34.1656	0.0258 +/- 0.0003
34.1354	0.0243 +/- 0.0003
34.1105	0.0226 +/- 0.0003
34.0912	0.0216 +/- 0.0003
34.0767	0.0200 +/- 0.0003
34.0664	0.0189 +/- 0.0003
34.0585	0.0186 +/- 0.0003
34.0505	0.0176 +/- 0.0003
34.0443	0.0162 +/- 0.0003
34.0390	0.0159 +/- 0.0003
34.0340	0.0154 +/- 0.0003
34.0293	0.0143 +/- 0.0003
34.0252	0.0136 +/- 0.0003
34.0210	0.0131 +/- 0.0003
34.0170	0.0125 +/- 0.0003
34.0140	0.0120 +/- 0.0003
34.0131	0.0114 +/- 0.0003
34.0118	0.0111 +/- 0.0003
34.0098	0.0106 +/- 0.0003
34.0084	0.0103 +/- 0.0003
34.0077	0.0096 +/- 0.0003
34.0064	0.0096 +/- 0.0003
34.0058	0.0092 +/- 0.0003
34.0053	0.0092 +/- 0.0003
34.0052	0.0090 +/- 0.0003
34.0047	0.0086 +/- 0.0003
34.0045	0.0081 +/- 0.0003
34.0043	0.0088 +/- 0.0003
34.0040	0.0078 +/- 0.0003
34.0039	0.0083 +/- 0.0003
34.0036	0.0081 +/- 0.0003
34.0034	0.0069 +/- 0.0003
34.0028	0.0078 +/- 0.0003
34.0024	0.0071 +/- 0.0003
34.0022	0.0076 +/- 0.0003

34.0020	0.0072 +/- 0.0003
34.0019	0.0072 +/- 0.0003
34.0019	0.0072 +/- 0.0003
34.0016	0.0071 +/- 0.0003
34.0016	0.0075 +/- 0.0003
34.0015	0.0068 +/- 0.0003
34.0013	0.0063 +/- 0.0003
34.0012	0.0073 +/- 0.0003
34.0009	0.0064 +/- 0.0003
34.0005	0.0062 +/- 0.0002
34.0005	0.0061 +/- 0.0002
34.0002	0.0061 +/- 0.0002
34.0001	0.0057 +/- 0.0002
34.0000	0.0057 +/- 0.0002
33.9997	0.0055 +/- 0.0002
33.9996	0.0055 +/- 0.0002
33.9995	0.0056 +/- 0.0002
33.9994	0.0055 +/- 0.0002
33.9993	0.0049 +/- 0.0002
33.9993	0.0057 +/- 0.0002
33.9992	0.0054 +/- 0.0002
33.9992	0.0054 +/- 0.0002
33.9992	0.0049 +/- 0.0002
33.9990	0.0049 +/- 0.0002
33.9988	0.0044 +/- 0.0002
33.9986	0.0046 +/- 0.0002
33.9985	0.0042 +/- 0.0002
33.9984	0.0038 +/- 0.0002
33.9983	0.0039 +/- 0.0002
33.9982	0.0039 +/- 0.0002
33.9981	0.0036 +/- 0.0002
33.9979	0.0036 +/- 0.0002
33.9977	0.0034 +/- 0.0002
33.9973	0.0033 +/- 0.0002

DATA RUN 9

FILM THICKNESS 0.46 MICRONS

TEMPERATURE (C)	DELTA N
35.2484	0.0548 +/- 0.0016
35.1451	0.0482 +/- 0.0015
35.1446	0.0503 +/- 0.0015
34.9939	0.0505 +/- 0.0015
34.8678	0.0507 +/- 0.0015
34.6411	0.0442 +/- 0.0015
34.3684	0.0347 +/- 0.0015
34.2229	0.0299 +/- 0.0014
34.3232	0.0311 +/- 0.0014
34.3207	0.0347 +/- 0.0015
34.2697	0.0283 +/- 0.0014
34.2681	0.0321 +/- 0.0014
34.1693	0.0223 +/- 0.0014
34.1603	0.0230 +/- 0.0014
34.1389	0.0191 +/- 0.0014
34.1349	0.0184 +/- 0.0014
34.1307	0.0221 +/- 0.0014
34.1158	0.0207 +/- 0.0014
34.1153	0.0193 +/- 0.0014
34.1061	0.0188 +/- 0.0014
34.1061	0.0189 +/- 0.0014
34.1049	0.0212 +/- 0.0014
34.1018	0.0214 +/- 0.0014
34.0948	0.0177 +/- 0.0014
34.0883	0.0175 +/- 0.0014
34.0817	0.0180 +/- 0.0014
34.0785	0.0159 +/- 0.0014
34.0785	0.0185 +/- 0.0014
34.0768	0.0167 +/- 0.0014
34.0738	0.0150 +/- 0.0014
34.0713	0.0159 +/- 0.0014
34.0711	0.0162 +/- 0.0014
34.0683	0.0161 +/- 0.0014
34.0667	0.0159 +/- 0.0014
34.0671	0.0134 +/- 0.0013
34.0650	0.0144 +/- 0.0014
34.0600	0.0147 +/- 0.0014
34.0586	0.0147 +/- 0.0014

DATA RUN 9

FILM THICKNESS 0.69 MICRONS

TEMPERATURE (C)	DELTA N
35.2484	0.0491 +/- 0.0013
35.1451	0.0444 +/- 0.0012
35.1446	0.0450 +/- 0.0013
34.9939	0.0407 +/- 0.0012
34.8678	0.0424 +/- 0.0012
34.4886	0.0356 +/- 0.0012
34.3684	0.0301 +/- 0.0012
34.3232	0.0261 +/- 0.0012
34.3207	0.0290 +/- 0.0012
34.2697	0.0253 +/- 0.0012
34.2681	0.0250 +/- 0.0012
34.2229	0.0229 +/- 0.0011
34.1693	0.0234 +/- 0.0011
34.1602	0.0201 +/- 0.0011
34.1389	0.0203 +/- 0.0011
34.1349	0.0210 +/- 0.0011
34.1307	0.0187 +/- 0.0011
34.1158	0.0186 +/- 0.0011
34.1153	0.0188 +/- 0.0011
34.1061	0.0177 +/- 0.0011
34.1061	0.0181 +/- 0.0011
34.1049	0.0183 +/- 0.0011
34.1018	0.0178 +/- 0.0011
34.0948	0.0163 +/- 0.0011
34.0883	0.0153 +/- 0.0011
34.0817	0.0134 +/- 0.0011
34.0785	0.0174 +/- 0.0011
34.0785	0.0143 +/- 0.0011
34.0785	0.0160 +/- 0.0011
34.0785	0.0137 +/- 0.0011
34.0768	0.0139 +/- 0.0011
34.0738	0.0140 +/- 0.0011
34.0713	0.0157 +/- 0.0011
34.0711	0.0142 +/- 0.0011
34.0683	0.0141 +/- 0.0011
34.0667	0.0165 +/- 0.0011
34.0667	0.0131 +/- 0.0011

34.0671	0.0168 +/- 0.0011
34.0671	0.0134 +/- 0.0011
34.0650	0.0168 +/- 0.0011
34.0650	0.0137 +/- 0.0011
34.0600	0.0119 +/- 0.0011
34.0586	0.0124 +/- 0.0011
34.0546	0.0155 +/- 0.0011
34.0546	0.0120 +/- 0.0011
34.0509	0.0120 +/- 0.0011
34.0443	0.0121 +/- 0.0011
34.0475	0.0115 +/- 0.0011
34.0473	0.0114 +/- 0.0011
34.0444	0.0124 +/- 0.0011
34.0442	0.0122 +/- 0.0011
34.0441	0.0121 +/- 0.0011
34.0440	0.0108 +/- 0.0011
34.0407	0.0106 +/- 0.0011
34.0402	0.0120 +/- 0.0011
34.0393	0.0114 +/- 0.0011
34.0373	0.0107 +/- 0.0011
34.0372	0.0103 +/- 0.0011
34.0361	0.0120 +/- 0.0011
34.0345	0.0107 +/- 0.0011
34.0343	0.0102 +/- 0.0011
34.0329	0.0100 +/- 0.0011
34.0322	0.0103 +/- 0.0011
34.0320	0.0108 +/- 0.0011
34.0280	0.0094 +/- 0.0011
34.0273	0.0089 +/- 0.0011
34.0272	0.0095 +/- 0.0011
34.0256	0.0089 +/- 0.0011
34.0236	0.0083 +/- 0.0011
34.0217	0.0073 +/- 0.0011
34.0196	0.0065 +/- 0.0011

DATA RUN 1

FILM THICKNESS 2.28 MICRONS

TEMPERATURE (C)	DELTA N
35.0508	0.0469 +/- 0.0008
34.7493	0.0418 +/- 0.0008
34.2594	0.0306 +/- 0.0007
34.1592	0.0255 +/- 0.0007
34.0892	0.0195 +/- 0.0007
34.0492	0.0158 +/- 0.0007
34.0258	0.0141 +/- 0.0007
34.0177	0.0130 +/- 0.0007
34.0133	0.0104 +/- 0.0006
34.0109	0.0100 +/- 0.0006
34.0064	0.0096 +/- 0.0006
34.0001	0.0079 +/- 0.0006
33.9958	0.0068 +/- 0.0006
33.9917	0.0054 +/- 0.0006

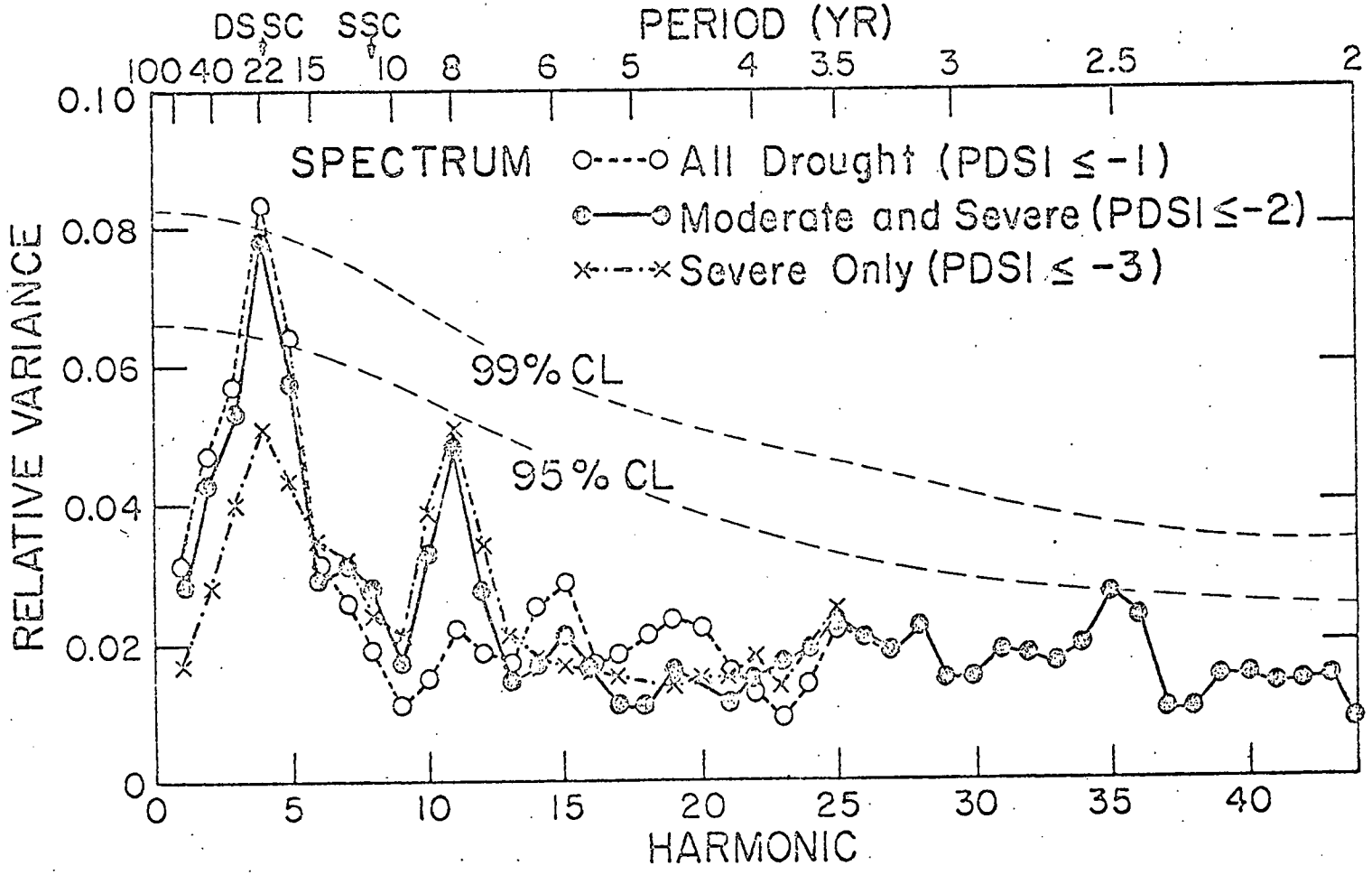
DS SC
SSC
PERIOD (YR)
100 40 22 15 10 8 6 5 4 3.5 3 2.5 2
0.10
0.08
0.06
0.04
0.02
0
RELATIVE VARIANCE
SPECTRUM
All Drought (PDSI ≤ -1)
Moderate and Severe (PDSI ≤ -2)
Severe Only (PDSI ≤ -3)
99% CL
95% CL
0 5 10 15 20 25 30 35 40
HARMONIC